Energy and AI 11 (2023) 100212

Contents lists available at ScienceDirect

Energy and AI

journal homepage: www.sciencedirect.com/journal/energy-and-ai

Consensus-based dispatch optimization of a microgrid considering meta-heuristic-based demand response scheduling and network packet loss characterization

Ali M. Jasim [a,b,*], Basil H. Jasim [a], Soheil Mohseni [c], Alan C. Brent [c,d]

[a] Electrical Engineering Department, University of Basrah, Basrah, 61001, Iraq
[b] Department of Communications Engineering, Iraq University College, Basrah, Iraq
[c] Sustainable Energy Systems, Wellington Faculty of Engineering, Victoria University of Wellington, Wellington, 6140, New Zealand
[d] Department of Industrial Engineering and the Centre for Renewable and Sustainable Energy Studies, Stellenbosch University, Stellenbosch, 7600, South Africa

HIGHLIGHTS

- A consensus-based microgrid dispatch optimization is presented.
- A multi-agent microgrid is conceptualized as a test-case system.
- Network packet losses are effectively characterized.
- Meta-heuristics are used to optimize the demand response capacity.
- The earth-worm optimization algorithm outperforms well-established meta-heuristics.

GRAPHICAL ABSTRACT

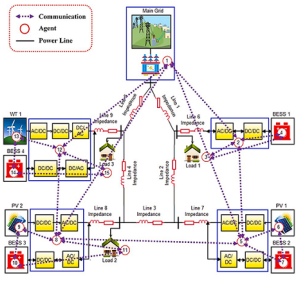

ARTICLE INFO

Keywords:
Demand-side management
Optimal scheduling
Microgrids
Distribution generation
Consensus algorithm
Meta-heuristics

ABSTRACT

The uncertainty inherent in power load forecasts represents a major factor in the mismatches between supply and demand in renewables-rich electricity networks, which consequently increases the energy bills and curtailed generation. As the transition to a power grid founded on the so-called grid-of-grids becomes more evident, the need for distributed control algorithms capable of handling computationally challenging problems in the energy sector does so as well. In this light, the consensus-based distributed algorithm has recently been shown to provide an effective platform for solving the complex energy management problem in microgrids. More specifically, in a microgrid context, the consensus-based distributed algorithm requires reliable information exchange with customers to achieve convergence. However, packet losses remain an important issue, which can potentially result in the failure of the overall system. In this setting, this paper introduces a novel method to effectively characterize such packet losses during information exchange between the customers and the microgrid operator, whilst solving the microgrid scheduling optimization problem for a multi-agent-based microgrid. More specifically, the proposed framework leverages the virulence optimization algorithm and the earth-worm optimization algorithm to optimally shift the energy consumption during peak periods to lower-priced off-peak hours. The effectiveness of the proposed method in minimizing the overall active power mismatches in the presence of packet losses has also been demonstrated based on benchmarking the results against the business-as-usual iterative scheduling algorithm. Also, the robustness of the overall meta-heuristic- and multi-agent-based method in producing

* Corresponding author.
E-mail address: e.alim.j.92@gmail.com (A.M. Jasim).

https://doi.org/10.1016/j.egyai.2022.100212

Available online 6 November 2022

optimal results is confirmed based on comparing the results obtained by several well-established meta-heuristic optimization algorithms, including the binary particle swarm optimization, the genetic algorithm, and the cuckoo search optimization.

1. Introduction

The ever-growing energy demand and the integration of non-dispatchable renewable energy resources (RERs) are increasingly contributing to the mismatches between generation and demand. Moreover, the uncertainty associated with power demand forecasts is one of the main drivers of supply-demand mismatches, which could lead to potentially significant load interruptions. The increasing electrification of various sectors is also contributing to this problem, especially in a power system with a high penetration of variable RERs.

Aimed at the cost-effective minimization of the mismatch of electricity supply and demand, demand-side management (DSM) using the flexibility potential of end-consumers is widely recognized as a technically feasible and economically viable tool [1–3]. In this context, smart integrated energy management solutions that are centered on the behaviors of end-users have been widely recognized to be particularly effective in reducing the system cost whilst improving reliability. In addition, an effective demand-side management strategy can shave off peaks in demand, and consequently improve the load factor. Particularly in microgrid settings, demand response solutions can significantly improve the self-sufficiency of the system. Accordingly, the associated DSM interventions provide an effective framework for end-consumers to participate in electricity markets and shift their non-critical loads to off-peak hours, thereby contributing to the flattening of the overall load profile [4].

In general, DSM solutions can be broadly classified into two classes of price- and incentive-based. More specifically, price-based load flexibility and control involve time-based pricing programs to reflect the time-variant wholesale electricity market prices in the customers' power bills. On the other hand, incentive-based demand response involves paying incentives to voluntary customers to interrupt their loads during higher-priced hours or when the reliability of the network is jeopardized. In this context, time-of-use (ToU) demand response frameworks have been found as one of the most effective demand-side management programs for reducing the operational costs of renewable and sustainable energy systems [5,6].

However, to effectively address the wider community-level power mismatches in such programs, effective communications between the load agents are necessary within an energy system's service territory. This brings to light the importance of multi-agent system-based modeling based on the consensus-based distributed algorithm to account for the associated community-level utility[1] dimensions [7–10]. More specifically, the so-called "consensus algorithm" refers to the set of distributed rules that govern the interactions between an agent and all of its neighbors. Such distributed rules are typically pre-programmed into the dedicated controllers responsible for communicating with nearby peers and identifying the locally optimum solutions [10,11].

Furthermore, it is increasingly recognized that optimizing the schedules of demand-side flexibility resources on a day-ahead basis can play a key role in finding the globally optimum operational costs of renewable and sustainable energy systems [5,8,10]. To this end, meta-heuristics have been shown to be particularly effective in lowering peak-to-average energy consumption ratios, thereby flattening the overall load profile and helping provide a better match between variable renewable energy generations and uncertain demands [1,3–5].

Moreover, there is a dire need to improve the economics and operational efficiency of grid-connected and isolated smart, integrated renewable energy systems, and particularly microgrids (MGs). Specifically, MGs have been frequently found to be not only central to the roll-out of variable RERs as part of global efforts to address climate change and energy decentralization, but also essential for accelerating universal energy access [2,3,8,9]. Accordingly, the consensus-based distributed control of the assets in MGs represents a cost-effective and reliable approach to coordinating increasingly decentralized ownerships.

More specifically, the consensus-based distributed dispatch of the resources in a MG context could offer several important advantages [10–12]: First, it can outperform centralized schemes in terms of the coverage area. This can mainly be explained by the fact that the consensus-based distributed algorithm relies on local data sharing between neighbors, whereas centralized approaches rely on high communication bandwidths to operate on system-wide data. Second, the consensus-based distributed approach reduces the associated communication costs. Importantly, such consensus-based distributed algorithms, which are centered on local data sharing between neighboring prosumers,[2] are expected to eliminate the need for high bandwidths needed in counterpart centralized algorithms. Third, future power grids and communication networks might have different topologies, which necessitates the plug-and-play functionalities offered by the consensus-based distributed approach. Such plug-and-play capabilities are necessary for the efficient handling of topological changes in power grids and communications networks. Finally, as a major risk factor, centralized systems are highly susceptible to a single point of failure because the entire system is dispatched from the main control center – a vulnerability that does not exist in distributed approaches. In other words, a decentralized network architecture is able to significantly reduce the vulnerability of the overall system to a single point of failure. Accordingly, consensus-based decentralized architectures allow the system to continue operating coherently even if multiple nodes fail at the same time.

In this light, this paper seeks to provide new layers of insight and understanding into the potentially significant role of consensus-based distributed algorithms for the optimal scheduling of renewable and sustainable energy systems, and particularly MGs. As mentioned above, the paper is additionally motivated by the need to: (i) minimize the network packet losses in the communications of load agents, and (ii) actively test the efficiency of meta-heuristic optimization algorithms for the globally optimal scheduling of multi-agent-based MGs – necessary for better reflecting reality.

1.1. Literature review

Table 1 provides an overview of the mainstream literature on the optimal scheduling of MGs. By identifying the overall objective, main findings, and limitations of the prior work, the table additionally lays the foundation for positioning the contributions of this study within the knowledge gaps.

A review of the literature has also identified the following main consequences of network power loss in smart integrated renewable energy systems, which attribute to the relevant data transmitted between the nodes on the instantaneous energy generation and consumption within the system [13]:

[1] The term "utility" in economics refers to the total satisfaction or benefit from consuming a good or service.

[2] A prosumer is a customer who both produces and consumes energy.

Table 1
Overview of the previous work.

Ref.	Overall objective	Main findings	Limitation(s)
[13]	A multi-agent consensus-based distributed energy management system considering the impact of packet losses	Minimizing the power mismatches and power bills	1) No consideration is given to demand-side management strategies.
[14]	Dispatch optimization of a MG based on the consensus algorithm	Minimizing the total operational costs and the supply-demand mismatches	1) The impact of communication network packet losses is ignored. 2) 2) No implementation of a demand response strategy.
[15]	Distributed energy management of a multi-agent MG using asynchronous consensus and distributed alternating direction multipliers	Minimizing the total operational costs	1) The impact of communication network packet losses is ignored. 2) No implementation of a demand response strategy.
[1]	Demand-side management based on the genetic algorithm, binary particle swarm optimization, and cuckoo search algorithm	Minimizing the peak-to-average ration and power bills	1) No consideration is given to using a graph network to transfer data between the MG agents. 2) The impact of communication network packet losses is ignored. 3) No robustness tests are undertaken.
[16]	Demand-side management based on the Newton Trust Region Method	Minimizing the total operational costs and the supply-demand mismatches	1) Integration of renewable energy sources is ignored. 2) Dynamic pricing and optimization algorithms are not adopted. 3) No consideration is given to using a graph network to transfer data between MG connect agents. 4) The impact of communication network packet losses is ignored.
[17]	Behavior-driven price-based Model Predictive Control for MG energy management	Minimizing the peak-to-average ration and power bills	1) Integration of renewable energy sources is ignored. 2) Dynamic pricing and optimization algorithms are not adopted. 3) No consideration is given to using a graph network to transfer data between the MG agents. 4) The impact of communication network packet losses is ignored.
[18]	Non-cooperative game-theoretic model for demand-side management	Minimizing the peak-to-average ratio, system costs, and end-users' discomfort	1) No consideration of the optimal trade-offs between renewable energy sources and storage devices. 2) No consideration is given to using a graph network to transfer data between the MG agents. 3) The impact of communication network packet losses is ignored.
[19]	Demand-side management based on the genetic algorithm and the bacterial foraging	Minimizing the peak-to-average ratio and system costs	1) No consideration is given to using a graph network to transfer data between the MG agents. 2) The impact of communication network packet losses is ignored. 3) On-site renewable energy and dynamic pricing are not used.
[20]	A coalition formation approach for the distributed energy exchange between the interconnected MGs	Maximizing the profits and minimizing the energy loss	1) No consideration is given to using a graph network to transfer data between the MG agents. 2) The impact of communication network packet losses is ignored. 3) No demand-side management strategy is implemented.
[21]	A game-theoretic framework for the distributed energy exchange between the interconnected MGs	Minimizing operational costs	1) No consideration is given to using a graph network to transfer data between the MG agents. 2) The impact of communication network packet losses is ignored. 3) No demand-side management strategy is implemented.
[22]	Demand-side management based on the whale optimization algorithm	Peak load reduction and energy savings	1) No consideration is given to using a graph network to transfer data between the MG agents. 2) The impact of communication network packet losses is ignored. 3) Integration of renewable energy sources is ignored, dynamic pricing.
[23]	Demand-side management based on the artificial fish swarm optimization	Minimizing the operational costs	1) No consideration is given to using a graph network to transfer data between the MG agents. 2) The impact of communication network packet losses is ignored.
[24]	Dispatch optimization of an islanded heat-electricity MG based on the consensus algorithm	Minimizing the total operational cost	1) The impact of communication network packet losses is ignored. 2) No implementation of a demand response strategy.
[25]	An optimal scheduling algorithm based on the distributed consensus algorithm	Minimizing the cost of dispatchable power generation and grid power imports	1) No consideration of demand-side management strategies.

(continued on next page)

Table 1 (*continued*)

Ref.	Overall objective	Main findings	Limitation(s)
[26]	A distributed energy management scheme for a DC MG using the consensus algorithm	Minimizing the electricity costs	1) The impact of communication network packet losses is ignored. 2) No consideration of demand-side management strategies.
[27]	A distributed energy management scheme for a DC MG using the consensus algorithm	Minimizing the electricity costs	1) The impact of communication network packet losses is ignored. 2) No consideration of demand-side management strategies.
[28]	A distributed consensus energy management algorithm with forecast tracking and trusted communication networks	Minimizing the electricity costs	1) The impact of communication network packet losses is ignored. 2) No consideration of demand-side management strategies.
[29]	Demand-side management based on the particle swarm optimization algorithm	Minimizing the peak-to-average ratio and electricity bills	1) Neglecting the user comfort standards. 2) No consideration is given to using a graph network to transfer data between the MG agents. 3) The impact of communication network packet losses is ignored.
[10]	A coalitional game-theoretic demand-side management framework	Minimizing power mismatches, power bills, and curtailed energy	1) Neglecting the user comfort standards. 2) No consideration is given to using a graph network to transfer data between the MG agents.
[30]	Demand-side management based on the strawberry optimization algorithm and particle swarm optimization	Minimizing electricity bills	1) On-site renewable energy technologies and backup storage systems are not used. 2) No consideration is given to using a graph network to transfer data between the MG agents. 3) The impact of communication network packet losses is ignored.
[31]	Dispatch optimization of a MG using the CPLEX solver	Minimizing supply-demand mismatches	1) No consideration is given to using a graph network to transfer data between the MG agents. 2) The impact of communication network packet losses is ignored. 3) No optimization-based demand scheduling framework.
[32]	Demand-side management based on the binary gray wolf optimization algorithm	Minimizing demand peaks and maximizing cost savings	1) No consideration is given to using a graph network to transfer data between the MG agents. 2) The impact of communication network packet losses is ignored. 3) No consideration of storage devices in the optimal scheduling problem.
[33]	Demand-side management based on the artificial cell swarm optimization and wingsuit flying search algorithm	Minimizing supply-demand mismatches	1) On-site renewable energy and backup storage systems are not used. 2) No consideration is given to using a graph network to transfer data between the MG agents. 3) The impact of communication network packet losses is ignored.
[34]	Demand-side management based on the ant lion optimization algorithm	Minimizing the power bills and the peak-to-average ratio	1) On-site renewable energy and backup storage systems are not used. 2) No consideration is given to using a graph network to transfer data between the MG agents. 3) The impact of communication network packet losses is ignored.

1) Transient instability in renewables-rich power systems during the transmission of data, which necessitates cost-prohibitive compensators.
2) Failure to meet the comfort levels of the end-users or loss of load due to discrepancies between the estimated and actual active electricity demand, as well as the deviation of voltage from the desired values.
3) Increased probability of demand-supply imbalances in the presence of a high share of variable renewables, which necessitates capital-intensive energy storage systems.
4) The possibility of additional costs charged by the service provider to compensate for the cost of rectifying supply-demand mismatches due to network power losses.

In this setting, the packet losses associated with decentralized networks have remained an important issue, which can potentially result in the failure of the overall system. Accordingly, to effectively characterize such packet losses during information exchanges between the customers and the MG operator, whilst solving the MG scheduling optimization problem for a multi-agent system, fundamentally new approaches are increasingly needed.

1.2. Research gaps and contributions

A comprehensive review of the relevant literature indicates the following specific gaps in the literature:

1 Paucity of multi-agent system-based MGs where consumers can effectively communicate with each other, as well as the MG operator, to reduce the overall power bill.
2 Lack of insight and understanding into the effect of the communication network packet losses, which can lead to potentially significant energy waste.
3 Narrow focus on unlocking the flexibility potential of end-users in the presence of network packet losses during the MG scheduling optimization phase with the aim of minimizing the system-wide costs.

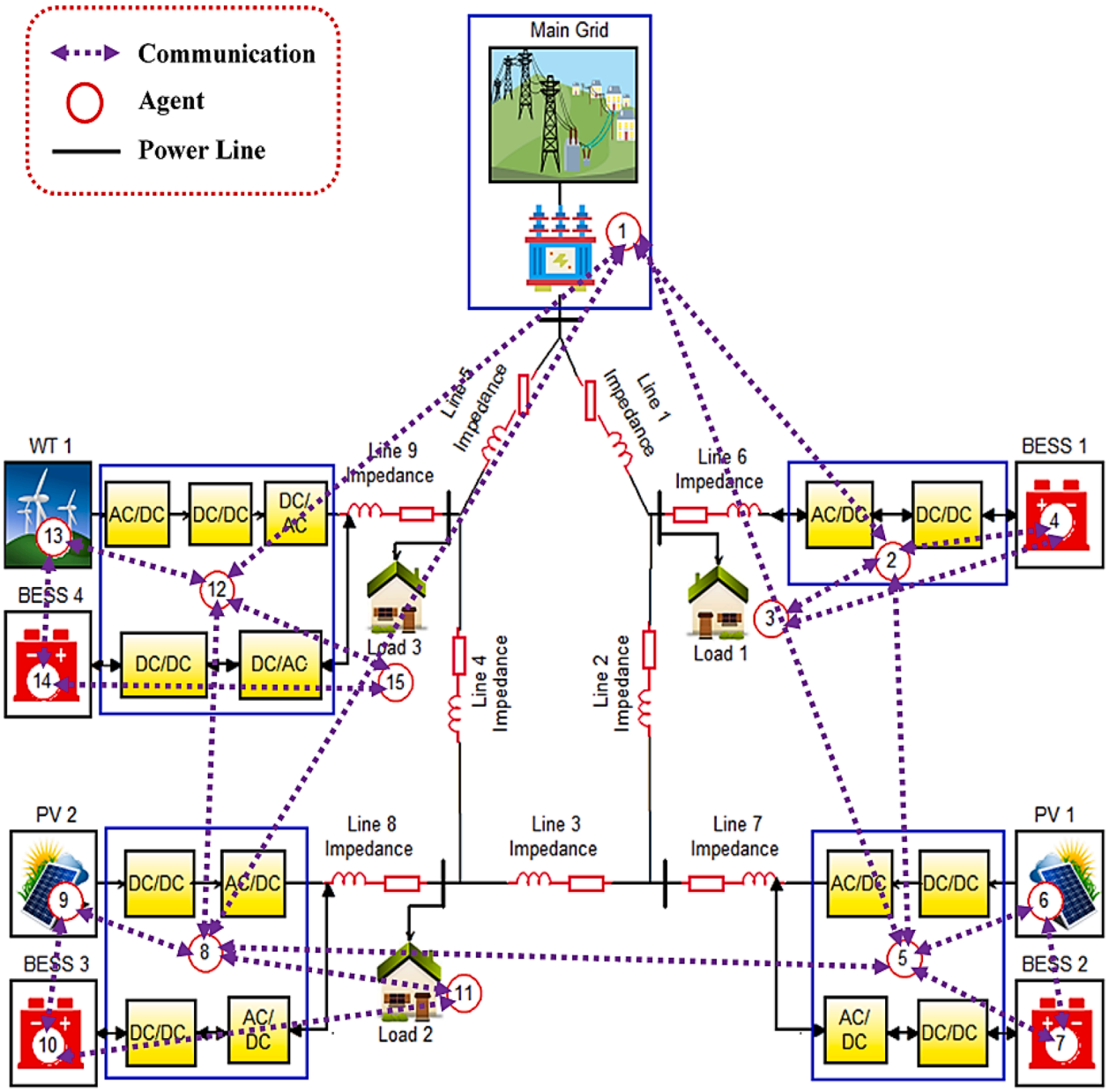

Fig. 1. Overall configuration of the proposed test-case MG.

4 Negligence of the potentially significant importance of some of the recently introduced meta-heuristics in nearing the globally optimum results for the MG dispatch optimization problem.

In response, this paper introduces a demand response-addressable, packet loss-aware MG operational scheduling method, which makes the following novel contributions, each addressing one of the identified gaps in the literature:

1 A new modeling framework is presented to enable the communication of load agents in a MG who seek the common goal of reducing the overall community-wide energy bills.
2 A network packet loss quantification model is presented for the first time in the literature to effectively characterize the associated packet losses during information exchanges between the customers and the microgrid operator, whilst solving the microgrid scheduling optimization problem.
3 A novel consensus-based distributed algorithm is combined with a meta-heuristic-based demand-side management strategy to determine the globally optimum microgrid dispatch in the presence of a pool of small-scale demand-side flexibility resources.
4 The performance of two recently introduced meta-heuristics, namely the virulence optimization algorithm (VBA) and the earthworm optimization algorithm (EWOA), are benchmarked against the well-established meta-heuristics in the literature.

To this end, for the first time in the literature, the proposed consensus-based distributed energy management algorithm tailored to multi-agent microgrids considering network packet losses, as well as demand-side flexibility resources optimized using the VOA and EWOA algorithms, simultaneously involves the following four modeling elements:

1 Minimizing the supply-demand mismatches;
2 Minimizing the overall system-wide operational costs;

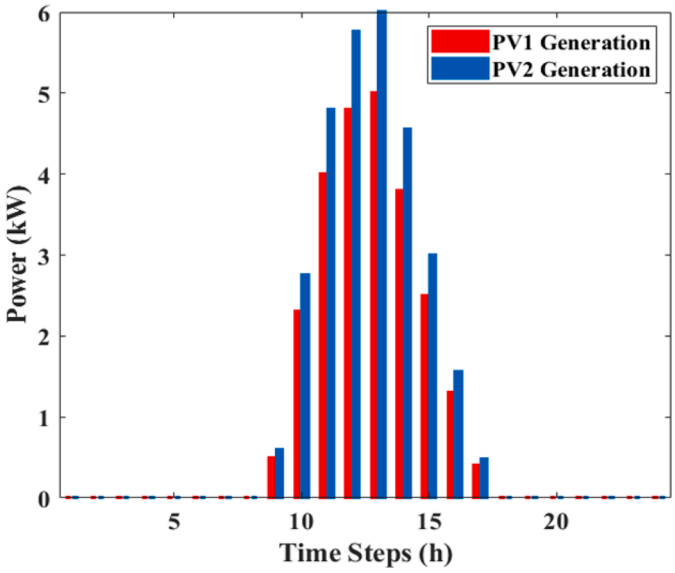

Fig. 2. Solar PV system's generation profile on the representative day.

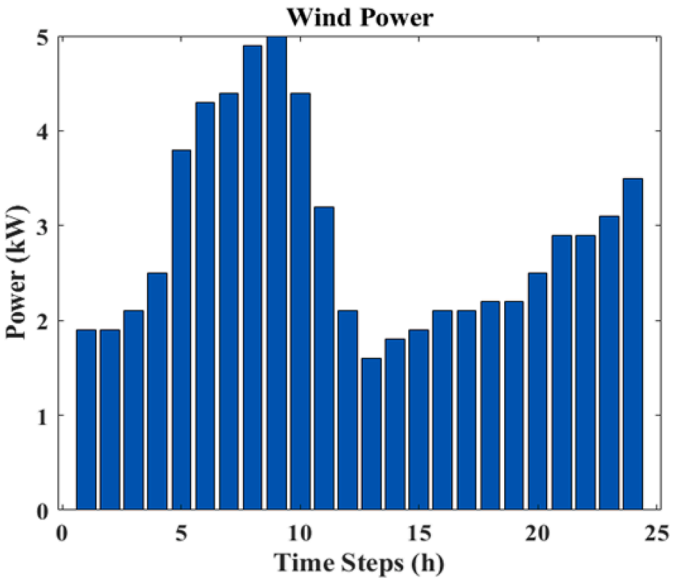

Fig. 3. Wind turbine's power generation profile on the representative day.

3 Minimizing the peak-to-average ratio of the load profile; and
4 Characterization of the network packet losses.

1.3. Paper organization

The rest of this paper is organized as follows. Section 2 presents the proposed test-case grid-connected MG. Section 3 formulates the consensus-based distributed energy management problem, while Section 4 presents the proposed methodology to solve the problem in the presence of network packet losses and demand-side flexibility resources. Subsequently, Section 5 presents the numeric simulation results obtained from the application of the proposed method to the test-case MG for a representative day of the system operation. Finally, Section 6 draws conclusions and presents areas for future work.

2. Proposed test-case grid-connected microgrid

In accordance with Fig. 1, the test-case grid-connected MG system integrates various RERs and storage devices. The following sub-sections present the mathematical models of the technologies considered for integration into the system.

2.1. Solar photovoltaic systems

The following equation can be used to model the power output from the solar photovoltaic (PV) system at each time-step of the system operation [35–37]:

$$P_s = P_{PV}^{nom}\frac{G}{G_{ref}}\left[1+K\left(T_{amb}+\left(\frac{NOCT-20}{800}G\right)-T_{ref}\right)\right], \tag{1}$$

where P_{PV}^{nom} represents the PV system's nominal power output under the standard test conditions, G denotes solar irradiance (W/m^2), G_{ref} (here, 1 kW/m^2) represents the reference solar irradiance, K represents the coefficient of power at different ambient temperatures, T_{amb} denotes the ambient temperature, $NOCT$ denotes the nominal operating cell temperature, while T_{ref} (here, 25 °C) is the reference temperature under standard test conditions.

Fig. 2 depicts the assumed daily solar PV production by the two existing installed systems considered. Specifically, the solar PV systems generate between the hours 9:00 a.m. and 5:00 p.m., which are then used to serve residential loads or stored in a battery bank, or a combination thereof. Accordingly, the optimization problem needs to effectively handle the residential loads when the solar PV system does not generate.

2.2. Wind turbine generator

The total power output from a wind turbine at each time-step of the system operation can be approximated as follows [38,39,40]:

$$P_{WT}(t)=\begin{cases} 0, & V(t)\le V_{cin} \text{ and } V(t)\ge V_{cout} \\ P_r^W, & V_{rat}\le V(t)\le V_{cout} \\ P_r^W\dfrac{V(t)-V_{cin}}{V_{rat}-V_{cin}}, & V_{cin}\le V(t)\le V_{rat} \end{cases} \tag{2}$$

where P_r^W denotes the rating power of a single wind turbine, V_{cin} denotes the cut-in wind speed, V_{rat} represents the rated wind speed, V_{cout} represents the cut-out wind speed, and $V(t)$ represents the reference height wind speed.

The following equation can also be used to normalize the wind speed recorded at the reference height to the wind turbine's hub height [38,41]:

$$V(t) = V_r(t)\left(\frac{H_{WT}}{H_r}\right)^{\lambda}, \tag{3}$$

where $V(t)$ denotes the wind speed normalized to the hub height H_{WT}, while $V_r(t)$ denotes the wind speed at the reference height H_r, and λ represents the friction coefficient. The coefficient of friction, λ, is typically equal to 1/7 for areas that are well-exposed and have smooth surfaces.

Accordingly, the assumed power generation output of the existing installed wind turbine on the representative day is illustrated in Fig. 3.

2.3. Energy storage system

The conceptualized MG employs a battery storage system to store energy when there is excess renewable power generation for use at times of power deficits. The state-of-charge (SOC) of the existing installed battery bank can be calculated in a continuous manner using the following equations [40,42,43]:

$$\frac{SOC(t)}{SOC(t-1)} = \int_{T-1}^{T}\frac{P_b(t)\eta_{batt}}{V_{bus}}dt, \tag{4}$$

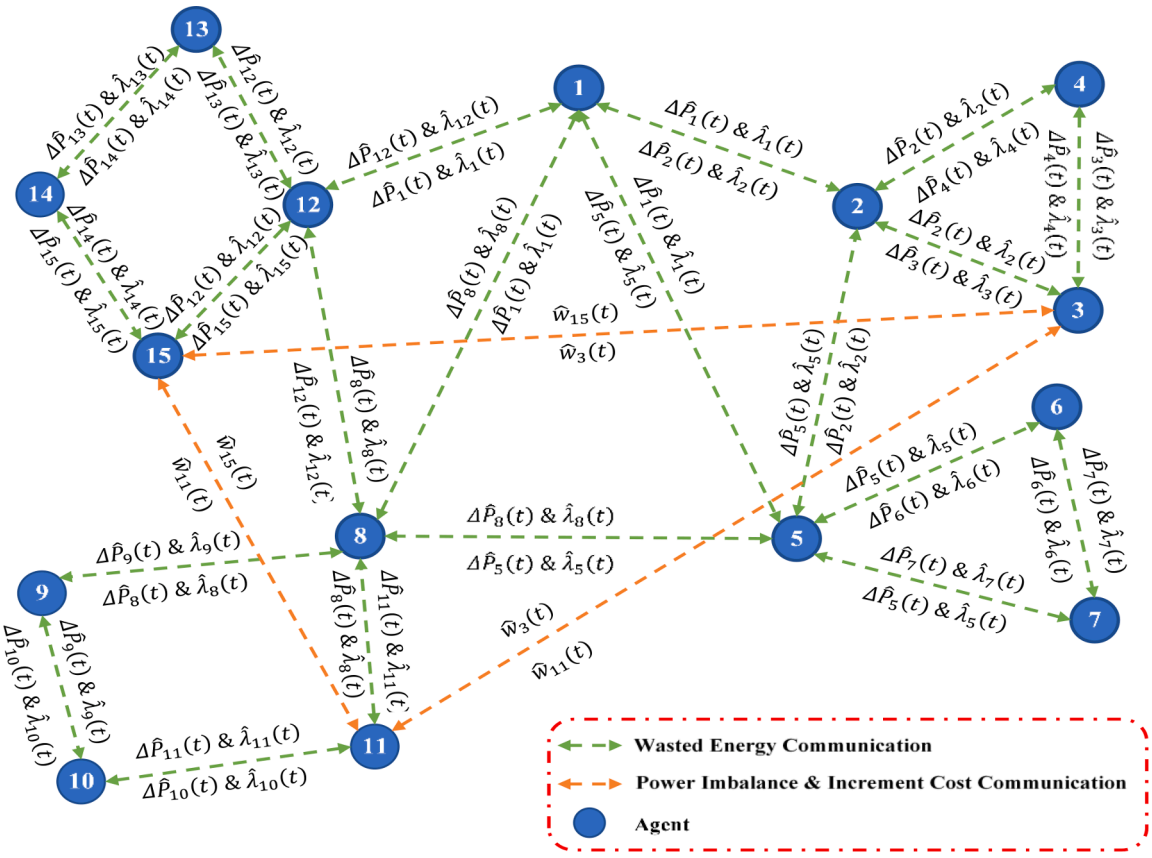

Fig. 4. Characterization of the information exchange between the agents.

where V_{bus} denotes the associated bus voltage, $P_b(t)$ denotes the battery's input/output power at time-step t, and η_{batt} represents the battery's round-trip efficiency. A positive sign for $P_b(t)$ indicates that it is in the charging mode; a negative, the discharging mode.

Also, the maximum allowable charge or discharge power of the battery is proportional to its maximum charge or discharge current, and can calculated as follows:

$$P_b^{max} = \frac{N_{batt} V_{batt} I_{max}}{1000}, \tag{5}$$

where I_{max} is the maximum charging current of the battery in Amperes, N_{batt} denotes the number of battery packs in the battery bank, and V_{batt} represents the voltage of each of the battery packs.

3. Consensus-based distributed energy management problem

3.1. Problem formulation

As discussed in the preceding section, the system of interest is a grid-connected MG, which integrates a set of renewable energy resources represented by $R \triangleq \{r_1, r_2, \ldots, r_R\}$, a set of energy storage devices represented by $B \triangleq \{b_1, b_2, \ldots, b_B\}$, and a set of load centers denoted by $L \triangleq \{l_1, l_2, \ldots, l_L\}$. The total number of generators, storage systems, and load centers is denoted by N. The algorithm for energy scheduling is formulated as an offline optimization problem, with the main objective of minimizing the overall community-wide electricity bill over the time horizon $T = \{1, 2, \ldots, T\}$ [44,45]:

$$min \sum_{t=1}^{T} PR(t) P_{grid}(t) \Delta t, \tag{6}$$

where $PR(t)$ is the energy price at time-step t, $P_{grid}(t)$ is the power purchased from the grid at time-step t, and Δt is the duration of each time-step.

The constraints on power balance Eq. (7), power rating Eqs. (8) and ((9)), and energy capacity (Eq. (10)) ensure that the simulated system adheres to the physical limitations as follows:

$$\sum_{l \in L} P_l(t) + \sum_{b \in B} P_b(t) + \sum_{r \in R} P_r(t) + P_{grid}(t) = 0, \ \forall t \in \tau \tag{7}$$

$$P_{b,\,min} \le P_b(t) \le P_{b,\,max}, \ \forall t \in \tau, \ \forall b \in B \tag{8}$$

$$0 \le P_{grid}(t) \le P_{grid,max}, \ \forall t \in \tau \tag{9}$$

$$E_b^{ini} - E_{b,\,max} \le \sum_{s=1}^{t} P_b(s) \Delta t \le E_b^{ini} - E_{b,\,min}. \ \forall t \in \tau, \ \forall b \in B \tag{10}$$

More specifically, the constraint in Eq. (7) ensures that the total power generation is equal to the total power consumption at each time-step, with the variables $l \in L$, $b \in B$, *and* $r \in R$ denoting a specific load center, storage device, and renewable energy generator, respectively. According to the constraints in Eqs. (8) and (9), the battery charge/discharge power and the import/export power must lie within a pre-defined range defined by the minimum and maximum charge capacities ($P_{b,\,min}$ and $P_{b,\,max}$) and the maximum grid power exchange capacity ($P_{grid,max}$) at each time-step. According to the constraint in Eq. (10), the amount of energy stored in the storage device $b \in B$ must, at all time-steps, lie within the pre-specified range defined by $E_{b,\,min}$ and $E_{b,\,max}$. Also, E_b^{ini} represents the total amount of energy stored in device b in the initial time-step of simulations.

3.2. Network model

It is assumed that every device in the MG is equipped with a

distributed controller, which enables communication with the peers in the service territory whilst making effective decisions for the local device. To characterize the communication network, an undirected graph, $G = \{V, E\}$ is used. More specifically, the vertices of the graph are denoted by $V = \{v_1, v_2, ..., v_N\}$, which are then used to represent the set of N controllers. Also, the set of edges connecting the neighboring controllers is denoted by $E \subset V \times V$. If any edge $(v_k, v_z) \in E$ in the graph also contains the inverse edge (v_z, v_k), then the graph can be referred to as an undirected graph. As mentioned above, in this paper, it is assumed that the communication network is undirected. That is, the network is assumed to have no single direction. Furthermore, for each edge $(k, z) \in E$ with $k, z \in V$, controller k receives data from controller z and vice versa. Moreover, the set of neighboring controllers of a controller $k \in V$ in the undirected graph G is denoted by $N_k = \{z : z \in V, (k, z) \in E\}$

As illustrated in Figs. 1 and 4, the proposed MG architecture and the associated communications network are comprised of a total of 15 agents. Specifically, the MG involves 4 independent distribution generators, 4 independent battery storage units, 1 wind turbine unit, 2 solar PV panel units, 1 main utility grid, and 3 load centers. Note that each distributed energy resource has a specific local controller.

Recall that the communications network, depicted in Fig. 4, is an undirected connected graph. Accordingly, the adjacency matrix $W = [\omega_{kz} S_{kz}]$ of the graph can be defined by the following parameters:

$$S_{kz} = \begin{cases} 1 \text{ if } (v_k, v_z) \in E \\ 0 \text{ if otherwise} \end{cases}$$

$$\omega_{kz} = \frac{1}{max_{k=1,2,...N}|N_k| + 1}$$

Also, the factor ω_{kz} is enforced to lie between 0 and 1 for the algorithm to converge. In addition, connectivity refers to the existence of a path between any two nodes or devices. Accordingly, there is connectivity between nodes in a graph if and only if there is a path, or a connected edge, from one node to another. In mathematical terms, if an edge with the definition $(v_k, v_z) \in E$ exists, then the node v_z is connected to the node v_k as a neighbor.

3.3. Packet loss in an information exchange

A Bernoulli process is used to model the loss of packets in the communication network [46]. Let the binary variable $b_{k-z}(n) = 0$ *or* 1 represent the status of packet loss on communication link $k \to z$ at iteration n. The probability of $b_{k-z}(n)$ can then be calculated as follows:

$$\begin{cases} P\{b_{k-z}(n) = 0\} = r_{k-z}, \\ P\{b_{k-z}(n) = 1\} = 1 - r_{k-z}, \end{cases} \tag{11}$$

where r_{k-z} denotes the packet loss rate associated with the link $k \to z$; $r_{k-z} = 1$ if $(k, z) \notin E$. It is noteworthy that by assigning distinct packet loss rates to different links, it can be ensured that the packet loss in the overall network is not uniform.

Let $\varsigma_k(n)$ represent the set of neighbors which have failed to deliver the information k at iteration n, and $\delta_k(n)$ represent the set of successful neighbors. Under these circumstances, the set of controller k's neighbors consists of $\varsigma_k(n)$ and $\delta_k(n)$, as $N_k = \varsigma_k(n) \cup \delta_k(n)$. Also, due to packet losses, controller k only updates with the received information set $\delta_k(n)$ at each iteration n, as the information set $\varsigma_k(n)$ is unavailable. Considering the associated packet losses, the following equations can be used to represent the general consensus-based updating rule [24]:

1) Power imbalance estimator [47]:

$$\begin{aligned} \Delta\widehat{P}_k^{n+1}(t) &= \Delta\widehat{P}_k^{n}(t) + \sum_{z \in N_k} \omega_{kz}\left(\Delta\widehat{P}_z^{n}(t) - \Delta\widehat{P}_k^{n}(t)\right) + P_k^{n+1}(t) - P_k^{n}(t) \\ &= \Delta\widehat{P}_k^{n}(t) + \sum_{z \in \delta_k(n)} \omega_{kz}\left(\Delta\widehat{P}_z^{n}(t) - \Delta\widehat{P}_k^{n}(t)\right) + P_k^{n+1}(t) - P_k^{n}(t), \ \forall t \in \tau \end{aligned} \tag{12}$$

where $\Delta\widehat{P}_k^n(t)$ denotes the estimated local power imbalance at time-step t, $P_k^n(t)$ denotes the local power exchange at time-step t, the factor $\omega_{kz} = \frac{1}{max_{k=1,2,...N}|N_k|+1}$, and N_k is the set of controller k's neighbors. Also, the iteration index is denoted by n, while the time interval for the finite schedule horizon $T \geq 1$ is denoted by $t \in [1, T]$.

2) Incremental cost estimator:

$$\begin{aligned} \lambda_k^{n+1}(t) &= \lambda_k^n(t) + \sum_{z \in N_k} \omega_{kz}\left(\lambda_z^n(t) - \lambda_k^n(t)\right) + \zeta\Delta\widehat{P}_k^n(t) \\ &= \lambda_k^n(t) + \sum_{z \in \delta_k(n)} \omega_{kz}\left(\lambda_z^n(t) - \lambda_k^n(t)\right) + \zeta\Delta\widehat{P}_k^n(t), \ \forall t \in \tau \end{aligned} \tag{13}$$

where $\lambda_k^n(t)$ is the local incremental cost estimation for time-step t, and ζ is a step size that is sufficiently small.

According to the consensus-based updating rule in Eq. (13), the local power imbalance estimation $\Delta\widehat{P}_k^n(t)$ is influenced by its neighbors' imbalances, $\Delta\widehat{P}_z^n(t)$ $(z \in N_k)$, at each iteration n. To account for the influence of neighbors at each iteration, an auxiliary variable $\chi_{k-z}^n(t)$ is used as follows:

$$\chi_{k-z}^n(t) = \begin{cases} \chi_{k-z}^{n-1}(t) + \omega_{kz}\left(\Delta\widehat{P}_z^{n-1}(t) - \Delta\widehat{P}_k^{n-1}(t)\right), \ if \ z \in \delta_k(n-1) \\ \chi_{k-z}^{n-1}(t), \ if \ z \in \varsigma_k(n-1) \end{cases} \forall t \in \tau \tag{14}$$

where $\delta_k(n-1)$ represents the set of neighbors that successfully deliver the packet to controller k at iteration $n-1$, and $\varsigma_k(n-1)$ represents the set of neighbors that fail to deliver the packet.

The auxiliary variable $\chi_{k-z}^n(t)$ represents the modifications that controller k has made to its variable $\Delta\widehat{P}_k^n(t)$ in accordance with the impact of its neighbor z before iteration n. Nevertheless, in view of the potential packet losses, $\chi_{k-z}^n(t)$ is not necessarily equal to $-\chi_{z-k}^n(t)$. Accordingly, an adjustment variable $e_{kz}^n(t)$ is defined to account for the local power imbalance estimation caused by packet losses as follows:

$$e_{kz}^n(t) = \chi_{k-z}^n(t) + \chi_{z-k}^n(t). \ \forall t \in \tau \tag{15}$$

More specifically, the variable $e_{kz}^n(t)$ represents the total amount of the modifications of the controller k in both directions of the link $(k, z) \in E$.

The proposed communication system depicted is in Fig. 4. Also, the auxiliary variable χ_{k-z}^n ($\chi_{k-z}^n(t)$, $t \in T$) has been integrated into the process of exchanging information. At each iteration n, the controller k requests its neighbors to provide it with the value of $\chi_{z-k}^n(t)$ $(z \in N_k)$. It then calculates $e_{kz}^n(t)$ for each link $(k, z) \in E$ in its territory. Accordingly, using the variable $e_{kz}^n(t)$, controller k is able to determine any mismatches caused by local packet losses. To maintain the accuracy of the power imbalance estimation, controller k updates its local power imbalance estimation $\Delta\widehat{P}_k^{n+1}(t)$ based on $e_{kz}^n(t)$.

More specifically, at each iteration n, the following steps are followed:

Step 1: Use Eq. (14) to update the neighbors' impact in accordance with the outcome of the most recent packet delivery.
Step 2: Share information with neighbors, including the consensus variables $\Delta\widehat{P}_k^{n-1}(t)$ and $\lambda_k^{n-1}(t)$, in conjunction with the most recent impact variable $\chi_{k-z}^n(t)$.
Step 3: Determine the adjustment variable $e_{kz}^n(t)$ to effectively account for the errors introduced by the most recent packet delivery as:

$$e_{kz}^n(t) = \begin{cases} \chi_{k-z}^n(t) + \chi_{z-k}^n(t), \ if \ z \in \delta_k(n-1) \\ 0, \ if \ z \in \varsigma_k(n-1) \end{cases} \forall t \in \tau \tag{16}$$

Step 4: Apply the modified rule to the consensus variables $\Delta\widehat{P}_k^n(t)$ and $\lambda_k^n(t)$:

$$\Delta\widehat{P}_k^{n+1}(t)=\Delta\widehat{P}_k^n(t)+\sum_{z\in\delta_k(n-1)}\omega_{kz}\left(\Delta\widehat{P}_z^{n-1}(t)-\Delta\widehat{P}_k^{n-1}(t)\right)+P_k^{n+1}(t)-P_k^n(t) - \sum_{z\in\delta_k(n-1)}e_{kz}^n(t),\forall t\in\tau \tag{17}$$

$$\lambda_k^{n+1}(t)=\lambda_k^n(t)+\sum_{z\in\delta_k(n-1)}\omega_{kz}\left(\lambda_z^{n-1}(t)-\lambda_k^{n-1}(t)\right)+\Delta\zeta\widehat{P}_k^{n-1}(t),\ \forall t\in\tau \tag{18}$$

Step 5: Adjust the auxiliary variable $\chi_{k-z}^n(t)$ at the end of each iteration:

$$\chi_{k-z}^n(t)=\begin{cases}\chi_{k-z}^n(t)-e_{kz}^n(t),\ if\ z\in\delta_k(n)\\ \chi_{k-z}^n(t),\ if\ z\in\varsigma_k(n)\end{cases}\ \forall t\in\tau \tag{19}$$

It is noteworthy that in the case of a bidirectional communication link (k, z), the controllers k and z apply the relevant adjustment variable separately. More specifically, to compensate for the impact of the packet loss on link k to z, controller k updates its adjustment variable $e_{kz}^n(t)$. Simultaneously, controller z updates the counterpart adjustment variable $e_{zk}^n(t)$ to account for the effect of the packet loss on link z to k. Recall that $e_{kz}^n(t)$ is not necessarily equal to $e_{zk}^n(t)$, and is controlled by the packet delivery results in both directions of the link.

Given the iterative nature of the proposed method, the auxiliary variable $\chi_{k-z}^n(t)$ can be re-written as follows at the end of each iteration n (after step 5):

$$\chi_{k-z}^n(t)=\sum_{s\in\Omega_{kz}(n)}\omega_{kz}\left(\Delta\widehat{P}_z^s(t)-\Delta\widehat{P}_k^s(t)\right),\ \forall t\in\tau \tag{20}$$

where $\Omega_{kz}(n)$ is the set of iterations in which the packets are successfully delivered in both the forward and backward directions of the link (k,z), and can be obtained as follows:

$$\Omega_{kz}(n)=\{s<n|k\ \in\delta_z(s)\ z\in\delta_k(s)\}, \tag{21}$$

Note that Eqs. (20) and (21) hold true if $n>0$; thus:

$$\chi_{k-z}^n(t)=\sum_{s\in\Omega_{kz}(n)}\omega_{kz}\left(\Delta\widehat{P}_z^s(t)-\Delta\widehat{P}_k^s(t)\right),\ \forall t\in\tau \tag{22a}$$

$$\chi_{z-k}^n(t)=\sum_{s\in\Omega_{kz}(n)}\omega_{kz}\left(\Delta\widehat{P}_k^s(t)-\Delta\widehat{P}_z^s(t)\right),\ \forall t\in\tau \tag{22b}$$

In the next iteration $(n+1)$, the values of $\chi_{k-z}^{n+1}(t)$ and $\chi_{z-k}^{n+1}(t)$ are updated as follows:

$$\chi_{k-z}^{n+1}(t)=\begin{cases}\chi_{k-z}^n(t)+\omega_{kz}\left(\Delta\widehat{P}_z^n(t)-\Delta\widehat{P}_k^n(t)\right),\ if\ z\in\delta_k(n-1)\\ \chi_{k-z}^n(t),\ if\ z\in\varsigma_k(n-1)\end{cases}\ \forall t\in\tau \tag{23}$$

and

$$\chi_{z-k}^{n+1}(t)=\begin{cases}\chi_{z-k}^n(t)+\omega_{kz}\left(\Delta\widehat{P}_k^n(t)-\Delta\widehat{P}_z^n(t)\right),\ if\ k\in\delta_z(n-1)\\ \chi_{z-k}^n(t),\ if\ k\in\varsigma_z(n-1)\end{cases}\ \forall t\in\tau \tag{24}$$

Also, the adjustment variable $e_{kz}^{n+1}(t)$ is updated as follows:

$$e_{kz}^{n+1}(t)=\begin{cases}\chi_{k-z}^{n+1}(t)+\chi_{z-k}^{n+1}(t),\ if\ z\in\delta_k(n)\\ 0,\ if\ z\in\varsigma_k(n)\end{cases}\ \forall t\in\tau \tag{25}$$

Substituting Eqs. (23) and (24) into Eq. (25) then gives:
The value of $\chi_{k-z}^{n+1}(t)$ is additionally updated as follows:

Table 2
Specifications of the modelled battery energy storage systems.

BESS no.	Rated capacity (kWh)	$P_{b,\ min}$	$P_{b,\ max}$	E_b^{ini}
BESS 1	5	-5	5	1
BESS 2	10	-5	5	1.5
BESS 3	5	-5	5	0.5
BESS 4	5	-5	5	0.5

Table 3
Determination of the loss of packets on each link.

Link	1→2	1→5	1→8	1→12	2→3
Packet loss	0.05	0.05	0.05	0.05	0.1
Link	3→4	4→2	2→5	5→6	6→7
Packet loss	0.1	0.1	0.1	0.15	0.15
Link	7→5	5→8	8→9	9→10	10→11
Packet loss	0.15	0.15	0.2	0.2	0.25
Link	11→8	8→12	12→13	13→14	14→15
Packet loss	0.2	0.2	0.25	0.25	0.25
Link	15→12				
Packet loss	0.25				

$$\chi_{k-z}^{n+1}(t)=\begin{cases}\chi_{k-z}^{n+1}(t)-e_{kz}^{n+1}(t),\ if\ z\in\delta_k(n)\\ \chi_{k-z}^{n+1}(t),\ if\ z\in\varsigma_k(n)\end{cases}\ \forall t\in\tau \tag{27}$$

Finally, substituting Eqs. (23) and (26) into Eq. (27) gives:

$$\chi_{k-z}^{n+1}(t)=\begin{cases}\chi_{k-z}^n(t)+\omega_{kz}\left(\Delta\widehat{P}_z^n(t)-\Delta\widehat{P}_k^n(t)\right),\ if\ z\in\delta_k(n)\ and\ k\in\delta_z(n)\\ \chi_{k-z}^n(t),\ Otherwise\end{cases}\ \forall t\in\tau \tag{28}$$

When the proposed packet loss-aware, consensus-based iterative algorithm converges to the unique solution, there no longer exists any mismatch between the total power supply and the total demand. Mathematically, this can be expressed as follows:

$$\lim_{k\to\infty}\sum_{l\in L}P_l^k(t)+\sum_{b\in B}P_b^k(t)+\sum_{r\in R}P_r^k(t)+P_{grid}^k(t)=0.\ \forall t\in\tau \tag{29}$$

In this setting, Table 2 presents the specifications of the modelled battery energy storage systems (BESSs), including the rated capacity, minimum and maximum allowable power ratings, and the initial energy in-store. Also, the assumed values for the packet loss rate on the network's links are given in Table 3. The consideration of different packet loss rates for the network's communication links ensures that packet

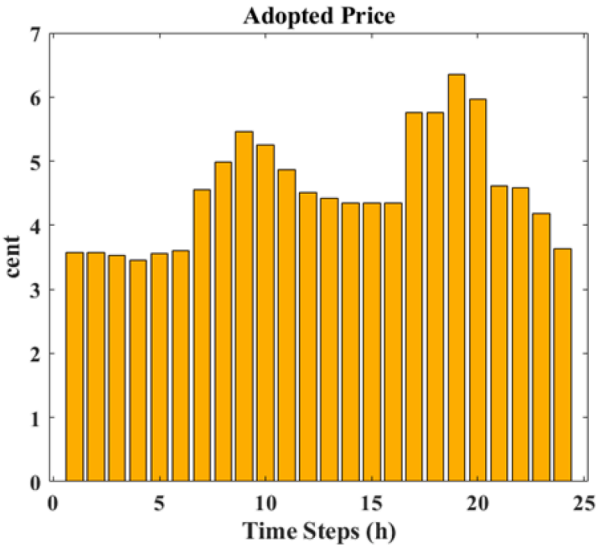

Fig. 5. ToU electricity tariff profile for the representative day.

losses are non-unified.

4. Adaptive consensus-based distributed energy management

This section presents the proposed demand-side management model for residential end-users within the MG's service territory who have on-site RERs and energy storage devices. More specifically, the model is centered on an adaptive consensus-based distributed energy dispatching algorithm. Recall that the main advantage of the proposed consensus-based approach compared to counterpart centralized approaches is allowing for local communications and sharing energy amongst neighboring agents necessary for improved resilience, self-sufficiency, and security of supply.

To further improve the efficiency of the proposed method, a demand response scheme is integrated into the model, which optimally schedules the supply of loads within the customers' comfort constraints. To this end, the model is developed based on the time-of-use (ToU) pricing scheme. To illustrate, Fig. 5 shows the tariffs considered in the simulations. Also, to minimize the peak-to-average energy consumption profile, the VOA and EWOA meta-heuristics are used (see the Appendix for the pseudo-codes). The meta-heuristic-based load flexibility scheme is then nested within the outer consensus-based distributed algorithm.

Assume a residential load with $l_u = \{m_1, m_2, \ldots, m_M\}$ appliances, where u is the load number ($u = 1, 2, \ldots, L$); $|l_u| \in$ M (total number of appliances considered). Also assume that there are two broad load types, namely: shiftable loads and non-interruptible loads. The washing machine, clothes dryer, electric water heater, and electric vehicle can, for example, be included in the set of shiftable loads. On the other hand, the set of non-interruptible loads can, for example, include refrigerators and lighting loads. After running the demand-side response program, shiftable appliances can be curtailed if it is profitable for the customer to do so. The end-user's objective is then to maximize the profit that can be achieved by curtailing the interruptible loads subject to the associated comfort standards.

In this context, assume that $\partial_{mi,h}$ represents a set of shiftable appliances operating at time-step h, with non-interruptible appliances served perfectly. Also, assume that each shiftable appliance can complete its task within a 24-hour time window. Accordingly, each shiftable appliance can tolerate a certain period of delay, φ_{mi}, as follows:

$$\varphi_{mi} = 24 - \alpha_{mi}, \tag{30}$$

where α_{mi} represents the acceptable comfort standard associated with the mi-th appliance, with Eq. (31) defining the upper and lower bounds of φ_{mi}:

$$\varnothing_1 \leq \varphi_{mi} \leq \varnothing_2, \tag{31}$$

where $\varnothing_1 = 24 - \alpha_{max}$ and $\varnothing_2 = 24 - \alpha_{min}$.

Also, the total demand in the baseline scenario can be obtained as follows:

$$\mathrm{E}_T = \sum_{i=1}^{M} \sum_{h=1}^{24} \mathrm{E}_{mi,h}. \tag{32}$$

Furthermore, the daily renewable power generation by the customers' on-site renewable energy generators can be expressed as:

$$\mathrm{E}_{RER} = \sum_{h=1}^{24} \mathrm{E}_{RER,h}. \tag{33}$$

In this setting, the customer's objective function for participation in the demand response program can be formulated as follows:

$$\min \left[\sum_{i=1}^{M} \sum_{h=1}^{24} E_{cost_{mi},h} \right], \tag{34}$$

subject to:

Table 4
Shiftable appliances and their usage specifications.

Appliance	Operating time	Rated power for load #1 (kW)	Rated power for load #2 (kW)	Rated power for load #3 (kW)
Washing machine	1:00–2:00 a.m. 10:00–11:00 a.m. 1:00–3:00 p.m.	2.25	1.15	1.15
Clothes dryer	1:00–5:00 a.m. 9:00–11:00 a.m. 7:00–9:00 p.m.	2.15	1.07	1.07
Electric vehicle	5:00–7:00 a.m. 9:00–10:00 a.m. 8:00 p.m.–0:00 a.m.	2.75	1.37	1.37
Water heater	4:00–9:00 a.m. 8:00 p.m.–0:00 a.m.	6.75	3.37	3.37

$$\mathrm{E}_{grid} = \sum_{i=1}^{M} \sum_{h=1}^{24} \mathrm{E}_{mi,h}, \forall BL \tag{35a}$$

$$\mathrm{E}_{grid,h} + \mathrm{E}_{RER,h} = \sum_{i=1}^{M} \sum_{h=1}^{24} \mathrm{E}_{T,h}, \forall IL \tag{35b}$$

$$\varphi_{max,\ mi} \leq 24 - \alpha_{mi}, \tag{35c}$$

$$\rho_{h,\ mi} \in \{0, 1\}. \tag{35d}$$

In the above formulation of the customer's payoff function (Eq. (34)), it is additionally assumed that the customer's non-interruptible energy demands are always satisfied using the on-site renewable energy resources and grid imports (Eq. (35a)). The maximum period of time that the consumption of any appliance can be shifted is also modelled using Eqs. (35b) and (35c), while the status of the appliance is modelled by a boolean variable that represents the fact that the appliance can either be ON or OFF at each time-step, as follows:

$$\rho_{h,\ mi} = \begin{cases} 0, & \textit{if appliance mi is OFF} \\ 1, & \textit{if appliance mi is ON} \end{cases} \tag{36}$$

Table 4 presents the timing and energy usage specifications of the shiftable loads considered in this study for the three end-point loads modelled.

As mentioned earlier, the proposed consensus-based distributed algorithm does not necessarily guarantee that the load factor – defined as the average load divided by the peak load – is maximized. This can consequently lead to excessive curtailments of surplus variable renewable power generations, and in turn, increased cost of energy.

To optimize the demand-side management optimization problem, formulated for the multi-agent MG considered, two state-of-the-art meta-heuristic optimization algorithms were used separately, namely the virulence optimization algorithm (VOA) and the earth-worm optimization algorithm (EWOA). Accordingly, Fig. 6 shows a flowchart of the overall consensus-based distributed algorithm that uses optimally shifted flexible loads.

In accordance with Fig. 6, the proposed DSM algorithm, which is fully integrated into the consensus-based distributed algorithm and is optimized using the VOA and EWOA algorithms, is run on an hourly basis to maximize the load factor and flatten the overall load profile. More specifically, to determine the optimum dispatch of demand response flexibility resources whilst adhering to the customers' comfort constraints, as well as finding the system-wide operating schedules for the dispatchable components, the objective function defined in Eq. (37) is minimized using the VOA and EWOA algorithms. The output of the optimization algorithm is the optimal dispatch of demand-side flexibility resources within the solution space defined by the comfort

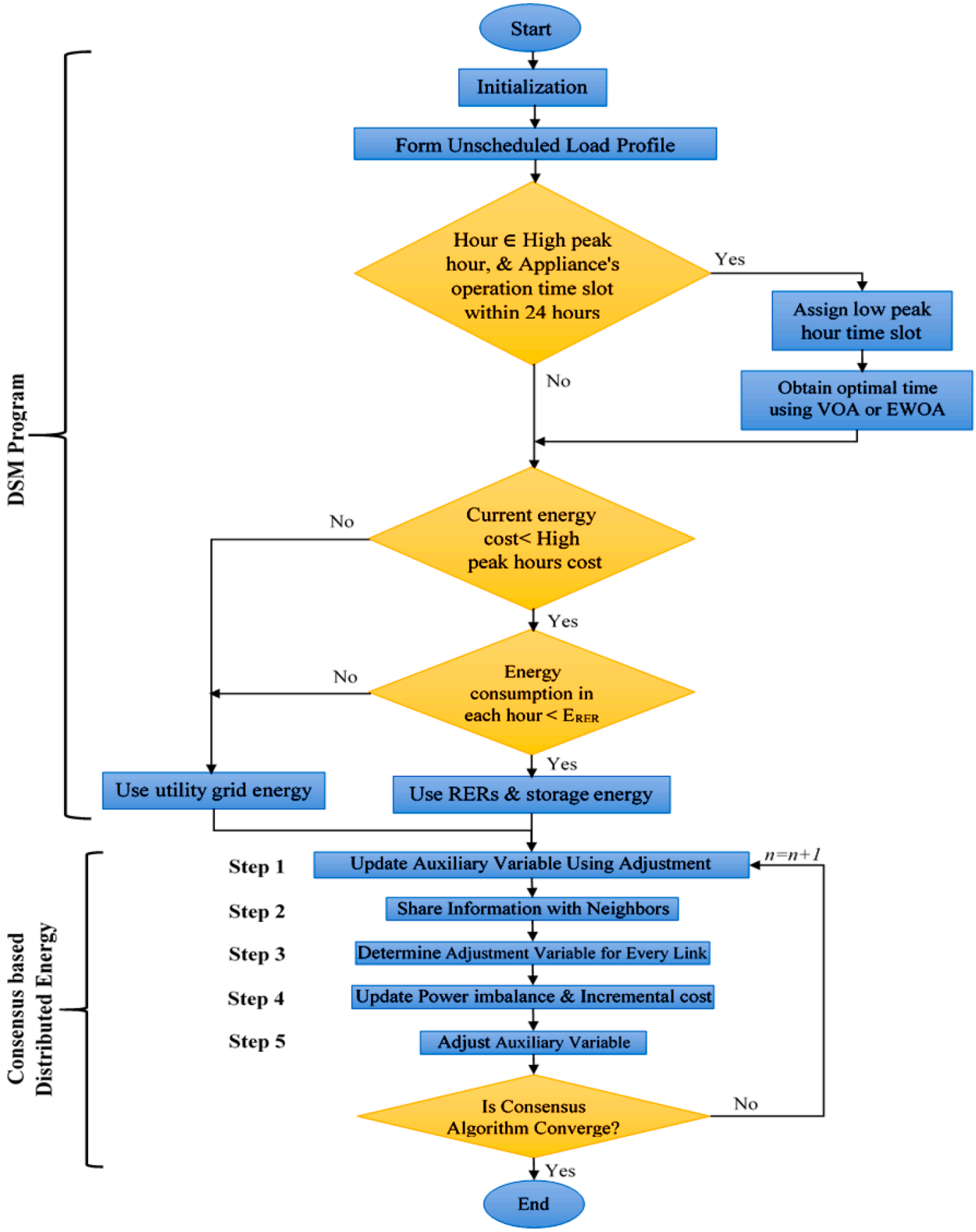

Fig. 6. Flowchart of the proposed consensus-based distributed algorithm for energy management.

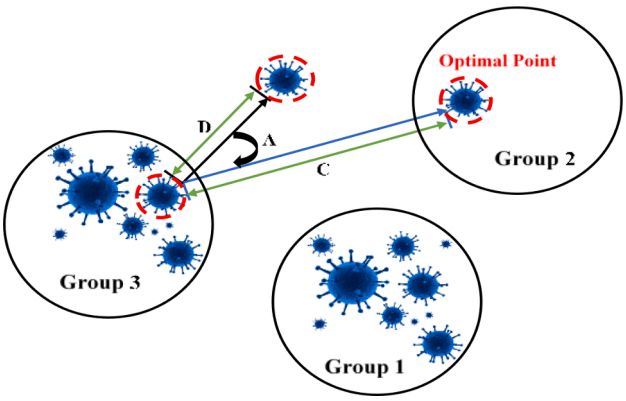

Fig. 7. Illustrating the escape mechanism of viruses in the VOA (adapted from [48]).

constraints of aggregated customers. Note that shiftable loads have been employed for the load flexibility program. Accordingly, the optimization problem shifts the loads to time periods that minimize the overall operating cost of the system.

Furthermore, for the real-world implementation of the optimal load flexibility schedules, specific devices can be installed at the customers' premises to monitor the consumption of end-use dispatchable resources and control their ON/OFF status using dedicated switches, in accordance with the signals received from the energy service provider.

The following two sub-sections provide an overview of the VOA and EWOA algorithms.

4.1. Virulence optimization algorithm

This VOA is inspired by mechanisms and functions with which viruses infect body cells, including virus recognition to invade body cells, reproduction (cloning) of these cells to initiate "invasion" of ready-to-infect regions, and egress from infected regions (to avoid immune reaction) [48]. The VOA, similar to the vast majority of evolutionary algorithms, starts with an initial population (here, viruses and host cells). The host cell population represents the resources available in the host environment – the region containing the globally optimum solution. The virus population then infiltrates the host environment and attempts to infect it. To this end, the viruses first reside in the formed regions, known as virus groups. The virus group with the highest mean fitness is then chosen as the first destination for the escape. Subsequently, the best viruses in each virus group are identified and cloned before the escape operation begins to spread the so-called virulence in the host environment. This process is repeated until the majority of the virus population is gathered in the region with the most resources, or in optimization terms, until reaching the global best solution.

It is noteworthy that when viruses live in a certain area, they typically tend to form virus groups or societies. Accordingly, in case of a movement to a better region, the group of viruses with the highest mean fitness value compared to other groups is normally chosen as the group to move. However, because the viruses are spread across the entire host region, it is hard to determine *a priori* to which group a virus belongs.

Accordingly, the *k*-means clustering technique is used in this algorithm to group viruses into a number of groups. Then, the mean fitness value of each group is calculated, and the group with the highest mean fitness is chosen as the escape point. The area around the fittest group is most likely to include the globally optimum solution. To increase the exploration power of the algorithm, when evading toward the destination, the viruses consider a deviation factor. Fig. 7 illustrates the escape mechanism of the viruses toward the selected group. As shown in the figure, the viruses with high fitness values travel the distance of "D" toward the globally optimum point with a deviation of "A" radians. In this way, the increased exploration power of the viruses enables them to search a wider area within the solution space necessary for locating potentially neglected resource-rich regions.

The escape mechanism plays a key role in ensuring that the algorithm converges to a unique solution. It is inspired by the relevant phenomena in nature, namely the vegetation of viruses in host environments and the fact that they favor hosts with weaker immune responses. More specifically, the escape mechanism has the following two notable advantages:

1 It permits mature viruses with greater fitness values to proliferate and infect the host environment. That is, it provides an effective platform for candidate viruses to search for regions with the highest resource density in the defined solution space. This process substantially increases the virulence probability of viruses within the host environment.
2 It blocks the immune system's ability to detect, clone, and neutralize mature viruses. Accordingly, when a virus is grown, reproduced, and mutated sufficiently, it can escape to a region with a greater possibility of survival, as well as more resources. The escape mechanism allows high-fitness viruses to rapidly reproduce and escape the infected area to a region before the immune system detects that resources are running low within a region and tries to kill the viruses living within the infected region.

The overall fitness function of the VOA for minimization subject to the constraints can be adapted for the demand-side management application of interest as follows:

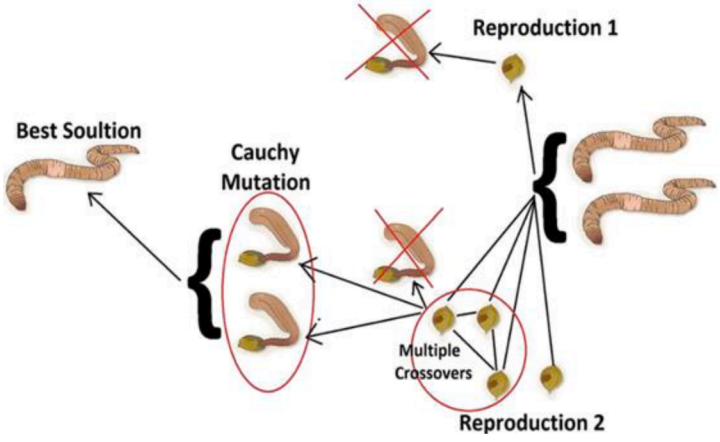

Fig. 8. Natural behavior of an earthworm (adapted from [55]).

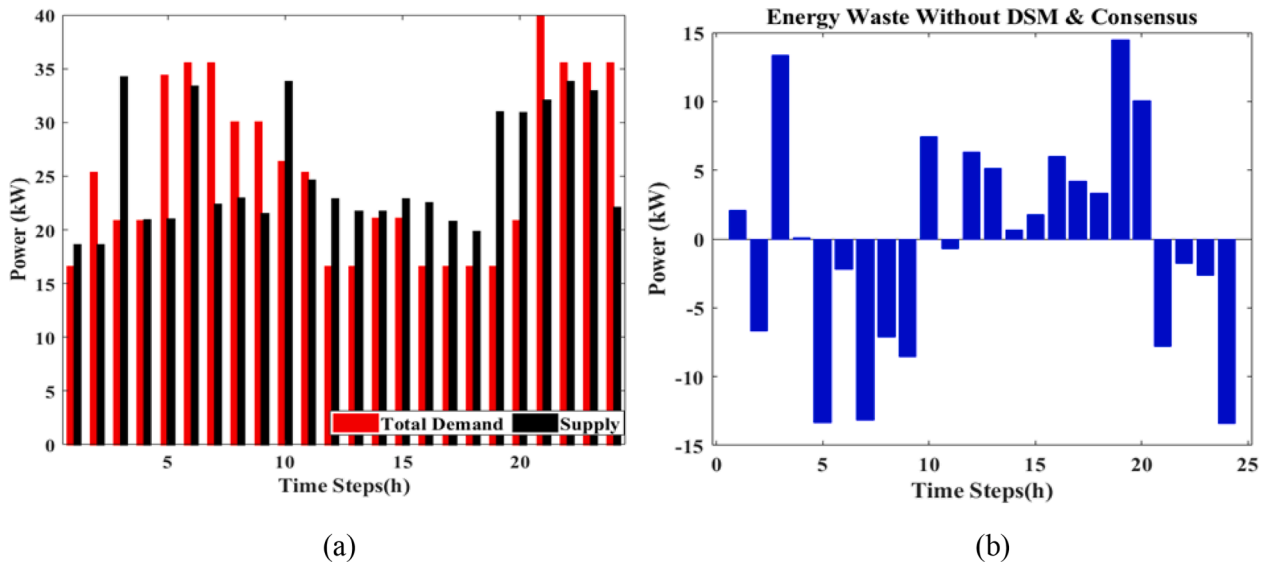

Fig. 9. Baseline scenario results: (a) supply and demand power profiles, and (b) power mismatch profile.

$$Fitness = \sum_{i=1}^{M} \sum_{h=1}^{24} \mathrm{E}_{mi,h}\, EP_h,\ \forall h \in \{1, 2, 3, \ldots\ldots, 24\} \tag{37}$$

where EP_h is the electricity price at time-step h, while M represents randomly initialized gene strands (problem solutions) with its length proportional to the number of residential electrical appliances.

At each iteration of evaluating the fitness function, viruses additionally undergo the crossover, mutation (drifting) and recombination (shifting) operators to increase the exploitation power of the algorithm [48–53]. Moreover, when two viruses compete for the same host cell, their genetic information is exchanged [52]. Based on comprehensive numerical simulations using small-scale test-case systems, it was decided to set the crossover rate (P_c) equal to 0.9. Accordingly, the mutation rate can be calculated as follows [52]:

$$Mutation\ Rate\ (P_m) = \frac{1 - P_c}{10}. \tag{38}$$

4.2. Earth-worm optimization algorithm

The EWOA is a new meta-heuristic algorithm, which is inspired by the living mechanisms of earthworms in nature [54]. The earthworms have two reproduction stages. Reproduction 1 produces only one offspring, whereas Reproduction 2 produces multiple offspring individuals at the same time. Accordingly, in the EWOA, multiple crossover operators are employed, with the overall value selected using the Cauchy Mutation operator. An abstract representation of an earthworm's natural behavior is shown in Fig. 8 [55].

In this study, the EWOA is developed using two natural earthworm breeding stages. The final earthworm is a weighted sum of the two offspring types, with the Cauchy Mutation operator used to select the overall value [56]:

$$W_j = \frac{\sum_{i=1}^{N_{pop}} x_{i,j}}{N_{pop}}, \tag{39}$$

where W_j represents the weight vector associated with the j-th element of population i, and N_{pop} is the population size.

Accordingly, the j-th earthworm's position can be found as:

$$x_{i,j}^{t+1} = x_{i,j}^{t} + CW_j, \tag{40}$$

where C denotes a random number returned from a Cauchy distribution with a scale parameter of 1.

The two reproduction types, modeled in this paper, are as follows [57]:

- **Reproduction 1**

Given the fact that earthworms are hermaphrodites, only a single earthworm can reproduce at a given time. The following equation models the offspring individuals produced by Reproduction 1:

$$x_{g1,i} = x_{max,i} + x_{min,i} - \alpha x_{g,i}, \tag{41}$$

where $x_{g,i}$ represents the i th element of the position of earthworm g, $x_{g1,i}$ denotes the i-th element of the newly spawned offspring earthworm $g1$, x_{max} and x_{min} are the upper and lower limits of the earthworm's position, respectively, and α represents a similarity factor between 0 and 1, which indicates the distance between the earthworm and its newly reproduced counterpart.

- **Reproduction 2**

Some earthworms have more than one offspring. This is modeled as Reproduction 2, which is a unique way for earthworms to reproduce. Specifically, the following equation yields the two offspring types utilized in the EWOA:

$$x_{12,i} = P_{1,i};\ x_{22,i} = P_{2,i},\ if\ rand\ >\ 0.5 \tag{42}$$

$$x_{12,i} = P_{2,i};\ x_{22,i} = P_{1,i},\ Otherwise$$

where $x_{12,i}$ and $x_{22,i}$ denote the i-th component of the two offspring types generated, with $P_{1,i}$ and $P_{2,i}$ denoting the i th elements of the two parents chosen for the uniform crossover operation.

Earthworms produced as part of Reproduction 2 can be classified using the following equation:

$$x_{g2} = \begin{cases} x_{12},\ if\ rand < 0.5 \\ x_{22},\ Otherwise \end{cases} \tag{43}$$

The earthworm produced as part of Reproduction 2 is then determined by the weighted sum of the two offspring earthworms as follows:

$$x_{g2} = w_1 x_{12} + w_2 x_{22}, \tag{44}$$

where w_1 and w_2 are specific weight factors.

Finally, the earthworm's final position in the next generation is

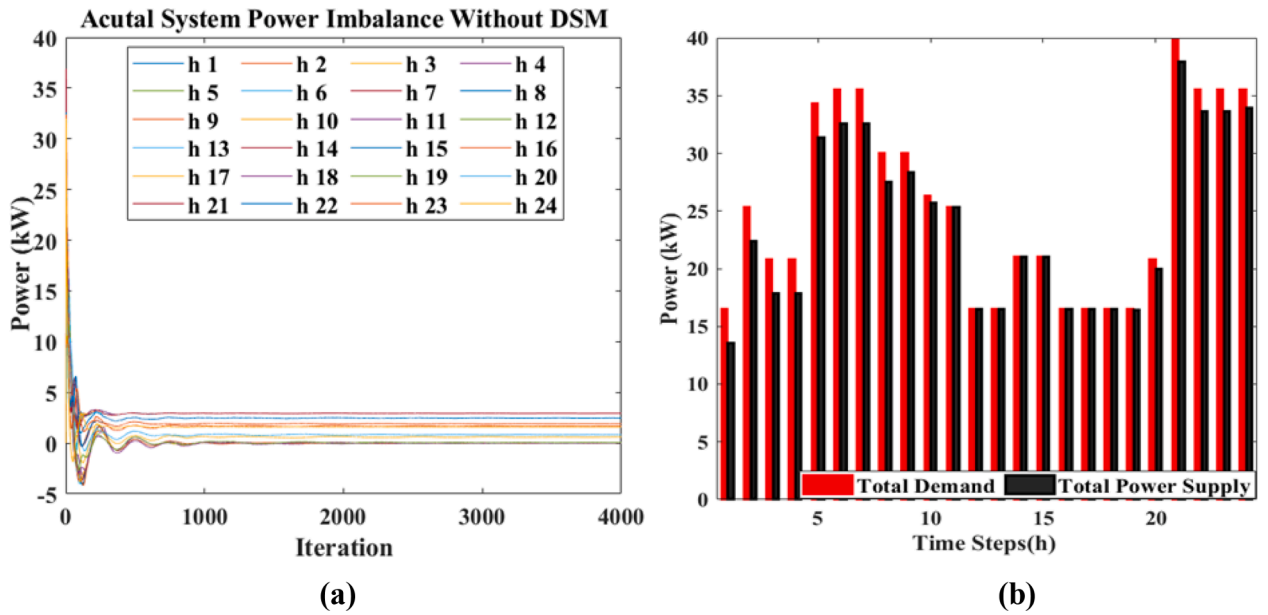

Fig. 10. Hourly profiles for: (a) the iterations of the power mismatch calculation process, and (b) the calculated supply-demand power mismatch using the consensus-based distributed algorithm.

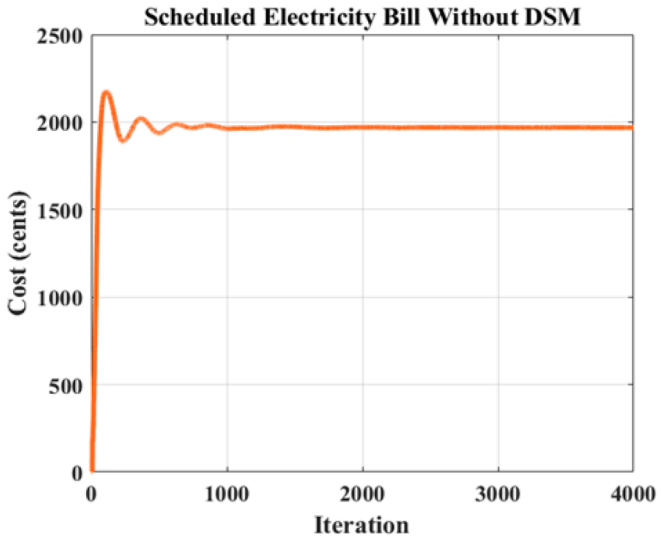

Fig. 11. Overall power bill for loads of interest.

determined by the following equation:

$$x_g^{t+1} = \beta x_{g1} + (1-\beta)x_{g2}, \tag{45}$$

where β is a specific proportional factor used to adjust the proportions of x_{g1} and x_{g2}, necessary for maintaining an adequate balance between the global and local search power.

5. Results and discussion

This section presents the numeric results from the simulation of the proposed method for the test-case of interest in MATLAB. To verify the robustness of the model to variations in input parameters for the representative day, three scenarios were defined, namely:

A Scenario 1: Baseline scenario without the consideration of responsive loads

B Scenario 2: Consensus-based distributed energy management without responsive loads

C Scenario 3: Consensus-based distributed energy management with the optimally scheduled responsive loads

5.1. Baseline scenario without the consideration of responsive loads

In this scenario, the simulation results without the consensus-based distributed algorithm and multi-agent system-based demand-side management are presented and discussed for the representative day. Fig. 9 summarizes the obtained results including the substantial supply-demand mismatches necessitating the significantly curtailed excess renewable power generation. Specifically, the positive power in Fig. 9 (b) shows the surplus power, whereas the negative power represents the renewable power deficit.

5.2. Consensus-based distributed energy management without responsive loads

This section presents the results of a scenario where the proposed consensus-based distributed energy management algorithm is used for the dispatch of the system of interest without scheduling the demand response capacity resources – using the proposed meta-heuristic-based scheduling algorithm. Fig. 10(a) depicts the convergence curve of the consensus-based distributed energy management algorithm for each hour of the representative day. Note that the proposed algorithm is run on an hourly basis, and accordingly, a separate convergence curve is produced for each hour of the representative day. Also, Fig. 10(b) depicts the supply-demand power mismatch at each hour. Furthermore, Fig. 11 shows the convergence process of the associated overall power bill for loads of interest.

Additionally, Fig. 12(a) depicts the difference between the surplus power and power deficit. As the figure shows, most of the hours of the day are associated with surplus power. The figure is also revealing in terms of significantly lower mismatches between generation and demand compared to Scenario 1. This verifies the effectiveness of the proposed consensus-based distributed algorithm in minimizing the mismatches in the presence of network packet losses. Moreover, Fig. 12 (b) shows the convergence curve of the proposed iterative method for

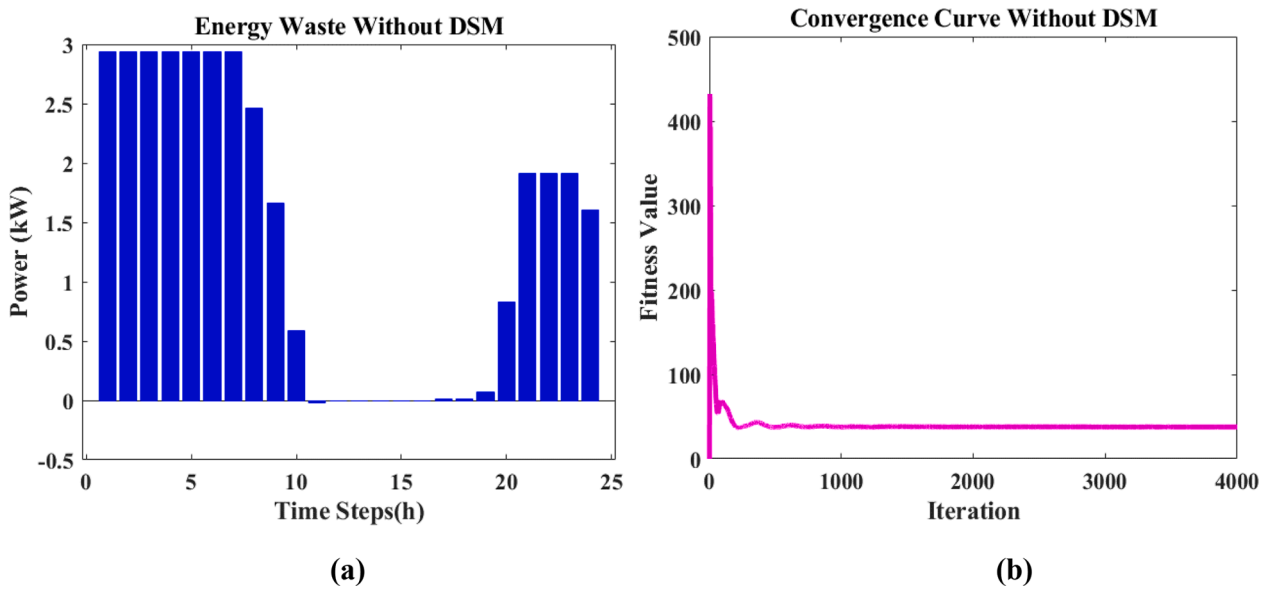

Fig. 12. Profiles for: (a) the hourly power mismatches, and (b) the daily convergence curve of the consensus-based distributed energy management scenario.

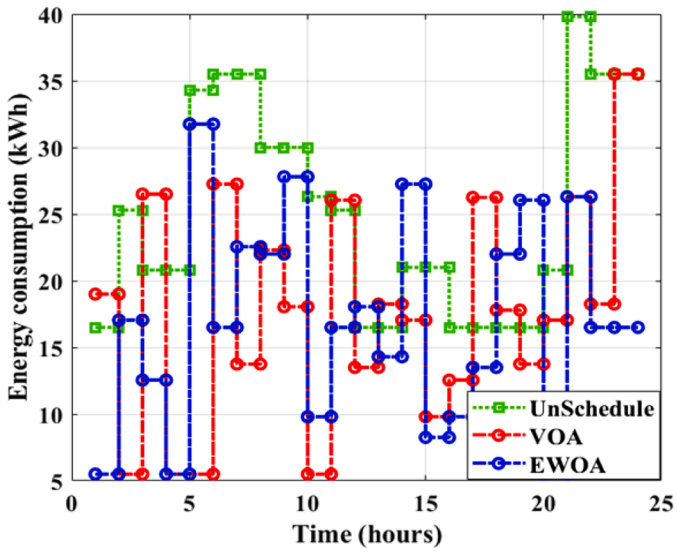

Fig. 13. Energy consumption profile for the representative day considering demand response.

the representative day, which indicates that there still exists a considerable mismatch between the overall generation and demand.

5.3. *Consensus-based distributed energy management with the optimally scheduled responsive loads*

Figs. 13-15 summarize the results of using the proposed consensus-based distributed energy management algorithm with the optimally scheduled responsive loads. As Fig. 13 shows, the optimal scheduling of responsive loads based on the proposed meta-heuristic-based algorithm considerably flattens the load curve compared to the scenario without using the flexibility potential of end-users. It can also be observed that both the VOA and the EWOA significantly smoothen out the load profile, albeit the impact of the EWOA is slightly more pronounced overall. This indicates that applying the proposed demand-side flexibility management algorithm has the potential to significantly reduce the electricity bill.

The convergence curve of the process used for the estimation of the power mismatch using the VOA is depicted in Fig. 14(a) for all the network nodes. Also, as Fig. 14(b) shows, any packet loss-driven supply-demand power mismatch has been eliminated. The node-specific convergence curve and the overall electricity bill produced by adopting the proposed consensus-based distributed algorithm and the VOA-optimized demand-side management are depicted in Fig. 14(c) and Fig. 14(d), respectively. As Fig. 14(d) shows, the overall power bill cost is reduced from $19.70 to $13.78, a significant 30% reduction.

Fig. 14 (e) shows the profile for surplus power and power deficit for the hours of the representative day, while Fig. 14(f) shows the associated convergence curve of the demand-side management algorithm. As Fig. 14(f) indicates, the fitness value has converged to 0 due to the elimination of any packet loss-driven supply-demand power mismatches.

5.3.1. *Comparison of meta-heuristics*

To show the robustness of the proposed method and measure the effectiveness of the VOA in nearing the globally optimum results, the performance of the VOA is compared with the EWOA, as well as a number of well-established meta-heuristics. Fig. 15 shows the simulation results for the consensus-based distributed energy management with the optimally scheduled responsive loads scenario, where the EWOA is used instead of the VOA. As the results indicate, the overall power bill is reduced to $12.05 from the $13.78 yielded by the VOA – a further 12.5% reduction.

Other algorithms, such as the genetic algorithm (GA), binary particle swarm optimization (BPSO), and cuckoo search (CS) have also been embedded within the overall framework, and have been found to reduce the electricity bill to $15.51, $14.47, and $16.67 respectively, compared to the base-case scenario. Accordingly, the overall power bill savings are as follows for the tested meta-heuristics: VOA = 30%, EWOA = 38.8%, GA = 21%, BPSO = 26.54%, and CS = 14.8%. This shows the significant potential of newly introduced meta-heuristics, particularly the VOA and the EWOA, in finding the globally optimum results for the demand response-addressable energy management problem in the presence of network packet losses.

6. Conclusions and future work

This paper has proposed a novel demand-side management modeling framework for grid-connected microgrids. The proposed framework uses a novel consensus-based distributed algorithm for effective packet loss-

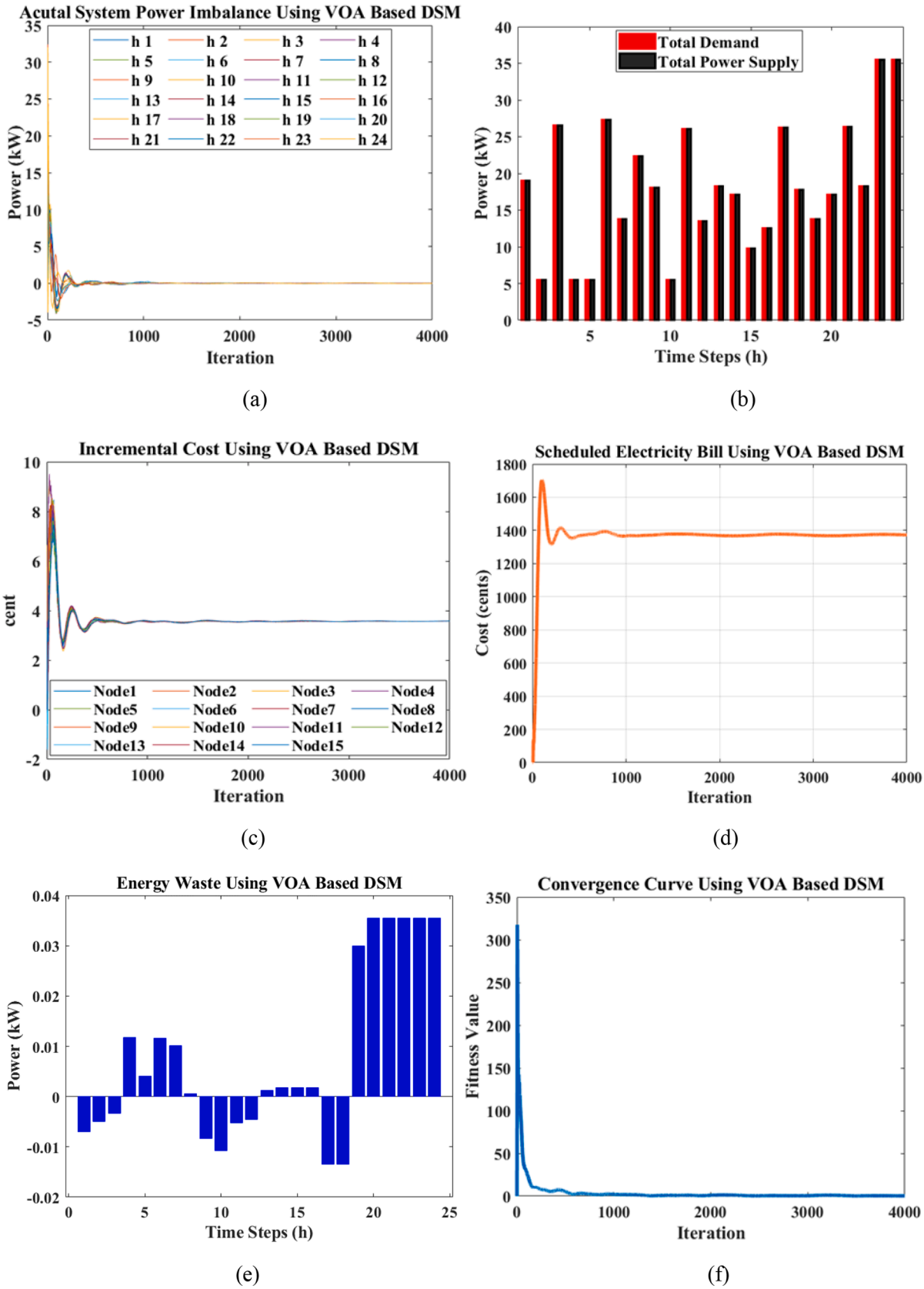

Fig. 14. Profiles for: (a) node-specific power imbalance estimation convergence curves, (b) supply-demand power mismatches, (c) node-specific power bill estimation convergence curves, (d) the overall power bill convergence curve, (e) hourly power mismatches, and (f) the convergence curve of the demand-side management algorithm for the consensus-based distributed energy management based on the VOA-optimized responsive loads.

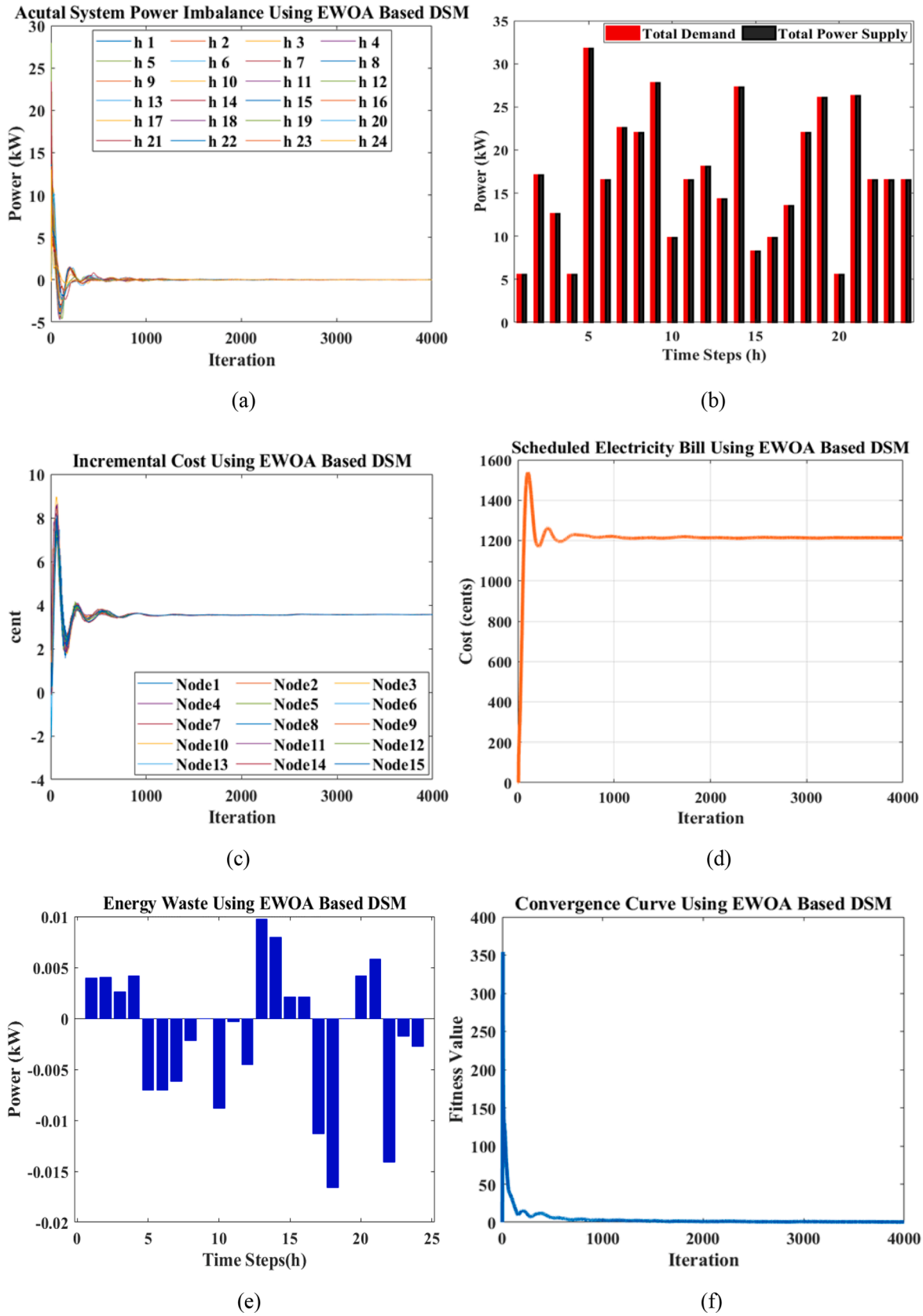

Fig. 15. Profiles for: (a) node-specific power imbalance estimation convergence curves, (b) supply-demand power mismatches, (c) node-specific power bill estimation convergence curves, (d) the overall power bill convergence curve, (e) hourly power mismatches, and (f) the convergence curve of the demand-side management algorithm for the consensus-based distributed energy management based on the EWOA-optimized responsive loads.

aware energy management, whilst optimally scheduling available demand response resources using state-of-the-art meta-heuristic optimization algorithms. The consensus-based distributed algorithm enables local communication between the neighboring load agents, thereby improving the accuracy of the characterization of network packet losses. Also, the recently introduced virulence optimization algorithm (VOA) and earthworm optimization algorithm (EWOA) are separately employed to solve the formulated demand-side management problem, which effectively shifts the energy consumption from peak to off-peak hours. The application of the proposed method to a hypothetical test-case system for a representative day has verified its effectiveness in nearing the globally optimum results for the demand response-addressable, packet loss-aware microgrid operational scheduling problem. More specifically, the proposed method's utility in reducing the mismatch between total generation and demand, and in turn, the overall power bill, has been demonstrated.

To validate the robustness of the proposed method, as well as to show the importance of using newly introduced meta-heuristics in microgrid scheduling applications, the results are compared with those obtained from the application of the model counterparts that use well-established meta-heuristics in the literature, namely the genetic algorithm (GA), the binary particle swarm optimization (BPSO), and the cuckoo search (CS) techniques. Accordingly, the following rank order has been found for the evaluated algorithms: the EWOA > the VOA > the BPSO > the GA > the CS. In terms of the impact on power bills, this equates to the following savings generated by each algorithm compared to the base-case scenario: EWOA = 38.8%, VOA = 30%, BPSO = 26.54%, GA = 21%, and CS = 14.8%. Additionally, a comprehensive comparison of several scenarios has further verified the validity of the results and the effectiveness of the proposed method for the microgrid scheduling problem in the presence of demand response and network packet losses. In conclusion, the results from this paper have provided new layers of insight and understanding into the importance of characterizing the network packet losses, unlocking the flexibility potential of end-users, and using state-of-the-art meta-heuristics for the "truly" optimal operation of grid-connected microgrids

Future work could seek to quantify various sources of uncertainty associated with the optimal micro-grid dispatching problem, including the forecasts of solar irradiance, ambient temperature, wind speed, power demand, and wholesale electricity prices. Another way of minimizing the so-called simulation-to-reality gaps could be to characterize the strategic interactions between various players in the system using game-theoretic methods. On a broader level, future work could seek to integrate the proposed optimal dispatch problem into the standard meta-heuristic-based optimal planning problem to formulate an integrated design and dispatch problem.

Declaration of Competing Interest

The authors declare that they have no known competing financial interests or personal relationships that could have appeared to influence the work reported in this paper.

Data availability

Data will be made available on request.

Appendix

This section provides the pseudo-codes of the virulence optimization algorithm (VOA) and the earth-worm optimization algorithm (EWOA), employed in the proposed method for the optimization of the demand response schedules (see Algorithm 1 and Algorithm 2).

Algorithm 1
Appliance Scheduling Algorithm Based on the VOA.

Require: popsize, maxgen, tbits, No. of clone, Pc, Pm
1: Generate initial population
2: initgeneration (popsize, tbits)
3: **for** $h = 1$ **to** 24 **do**
4: Evaluate the population and record current Fittest gene strand
5: [*best*] = Evaluatefitnessfunction (cost, popnew, popsize)
6: **if** $best_{mi} == 1$ **then**
7: $LOT_{mi} = LOT_{mi} - - 1$
8: **end if**
9: Search for gene strand optimal position in the entire search space
10: **for** $t = 1$ **to** m **do**
11: h = *findminimumcost (best, f(best), t)*
12: Shift to that hour the current best gene strand
13: **end for**
14: **if** $E_{cost}(h) < E_{max}$ **then**
15: **if** $E_{Tot,RES} > load_h$ **then**
16: Switch the load to RES storage system
17: **else**
18: Consume the grid energy
19: **end if**
20: **end if**
21: Generate new population
22: **for** $j = 1$ to *popsize* **do**
23: Select crossover pair
24: Select (a, b)
25: **if** $p_c > rand$ **then**
26: crossover (*a, b*)
27: **end if**
28: **if** $p_m > rand$ **then**
29: mutation (c, insite)
30: **end if**
31: New population generated, generate clones
32: popnew (popsize, tbits)
33: **end for**
34: *Validate − − constraints (popnew)*
35: **end for**

Algorithm 2
The EWOA.

1: **Procedure** START
2: **Initialization:** Generates counter of $t = 1$; Set P as the population of NP individual earthworms, which are randomly distributed in the search space; numbers of kept earthworms are set as nKEW, maximum generation MaxGn, α as similarity factor, proportional aspect β
3: **Evaluation of Fitness:** Each earthworm is evaluated individually according to its position
4: **while** *till best solution is not achieved or* $t <$ *MaxGen*
5: All the earthworms in the population are then sorted according to their fitness values
6: **for** $i = 1$ *to NP (all earthworms)* **do**
7: Generate offspring $xg_{1,i}$ through Reproduction 1
8: Generate offspring through Reproduction 2
9: **Do** crossover
10: **if** $i <$ *nKEW* ***then***
11: Set the number of particular parents (N) and the procured offsprings (M); Select N parents using the roulette wheel selection method; Generate M offsprings; Calculate $xg_{2,I}$ according to M offsprings generated
12: **else**
13: Randomly generate an individual earthworm as $xg_{2,i}$
14: **end if**
15: Update the location of earthworm i
16: **for** j = *nKEW 1 to NP (earthworm individuals non-kept)*
17: **do** Cauchy mutation
18: **end for**
19: Calculate the population according to the newly restructured positions
20: $t = t + 1$
21: **end while**
22: Best solution is extracted
23: **end**

References

[1] Javaid N, Ullah I, Akbar M, Iqbal Z, Khan FA, Alrajeh N, et al. An intelligent load management system with renewable energy integration for smart homes. IEEE Access 2017;5:13587–600.
[2] Yi P, Dong X, Iwayemi A, Zhou C, Li S. Real-time opportunistic scheduling for residential demand response. IEEE Trans Smart Grid 2013;4(1):227–34.
[3] Graditi G, Ippolito MG, Telaretti E, Zizzo G. Technical and economical assessment of distributed electrochemical storages for load shifting applications: an Italian case study. Renew Sustain Energy Rev 2016;57:515–23.
[4] Hubert T, Grijalva S. Modeling for residential electricity optimization in dynamic pricing environments. IEEE Trans Smart Grid 2012;3(4):2224–31.
[5] Rahimi F, Ipakchi A. Demand response as a market resource under the smart grid paradigm. IEEE Trans Smart Grid 2010;1(1):82–8.
[6] Alhasnawi BN, Jasim BH, Rahman Z-ASA, Siano P. A novel robust smart energy management and demand reduction for smart homes based on internet of energy. Sensors 2021;21:4756.
[7] Ozturk Y, Senthilkumar D, Kumar S, Lee G. An intelligent home energy management system to improve demand response. IEEE Trans Smart Grid 2013;4 (2):694–701.
[8] Ferruzzi G, Cervone G, Monache LD, Graditi G, Jacobone F. Optimal bidding in a Day Ahead energy market for micro grid under uncertainty in renewable energy production. Energy 2016;106:194–202.
[9] Peng T, Tomsovic K. Congestion influence on bidding strategies in an electricity market. IEEE Trans Power Syst 2003;18(3):1054–61.
[10] Alhasnawi BN, Jasim BH, Sedhom BE, Guerrero JM. Consensus algorithm-based coalition game theory for demand management scheme in smart microgrid. Sustain Cities Soc 2017;74:103248.
[11] Duan J, Chow M. A resilient consensus-based distributed energy management algorithm against data integrity attacks. IEEE Trans Smart Grid 2019;10:4729–40.
[12] Zhao C, Chen J, He J. Consensus-based energy management in smart grid with transmission losses and directed communication. IEEE Trans Smart Grid 2017;8: 2049–61.
[13] Dong X, Zhang X, Jiang T. Adaptive consensus algorithm for distributed heat-electricity energy management of an islanded microgrid. Energies 2018;11:2236.
[14] Zhao T, Ding Z. Distributed agent consensus-based optimal resource management for microgrids. IEEE Trans Sustain Energy 2018;9:443–52.
[15] Zheng Y, Song Y, Hill D, Zhang Y. Multi-agent system based microgrid energy management via asynchronous consensus ADMM. IEEE Trans Energy Conver 2018; 33(2):886–8.
[16] Gilda K, Chaphekar SN, Dharme AA, Talange DB. Demand side management in microgrids. In: 2018 International Conference on Emerging Trends and Innovations In Engineering And Technological Research (ICETIETR); July 2018.
[17] Mirakhorli A, Dong B. Model predictive control for building loads connected with a residential distribution grid. Appl Energy 2018;230:627–42.
[18] Fernandez E, Hossain MJ, Nizami MSH. Game-theoretic approach to demand-side energy management for a smart neighbourhood in Sydney incorporating renewable resources. Appl Energy 2018;232:245–57.
[19] Khalid A, Javaid N, Guizani M, Alhussein M, Aurangzeb K, Ilahi M. Towards dynamic coordination among home appliances using multi-objective energy optimization for demand side management in smart buildings. IEEE Access 2018;9: 19509–29.
[20] Essayeh C, El-Fenni M, Dahmouni H. Optimization of energy exchange in microgrid networks: a coalition formation approach. Protect Control Modern Power Syst 2019;4:24.
[21] C. Lahon R, Gupta C, Fernandez E. Coalition formation strategies for cooperative operation of multiple microgrids IET Gener Transm Distrib 2019;13:3661–72.
[22] Sharma A, Saxena A. A demand side management control strategy using Whale optimization algorithm. SN Appl Sci 2019;1:703–14.
[23] Kumar K, Saravanan B. Day ahead scheduling of generation and storage in a micro grid considering demand Side management. J. Energy Storage 2019;21:78–86.
[24] Duan J, Chow M. Robust consensus-based distributed energy management for microgrids with packet losses tolerance. IEEE Trans Smart Grid 2019;11:281–90.
[25] Tajalli S, Mardaneh M, Taherian-Fard E, Izadian A, Kavousi-Fard A, Dabbaghjamanesh M, et al. DoS-resilient distributed optimal scheduling in a fog supporting IIoT-based smart microgrid. IEEE Trans Ind Appl 2020;56:2968–77.
[26] Cheng Z, Chow M. Resilient collaborative distributed energy management system framework for cyber-physical DC microgrids. IEEE Trans Smart Grid 2020;11(6): 4637–49.
[27] Ullah M, Babaiahgari B, Alseyat A, Park J. A computationally efficient consensus-based multi-agent distributed EMS for DC microgrids. IEEE Trans Industr Electr 2020.
[28] Cutsem O, Dac D, Boudou P, Kayal M. Cooperative energy management of a community of smart-buildings: a blockchain approach. Int J Electr Power Energy 2020;117:105643.
[29] Cheng P-H, Huang T-H, Chien Y-W, Wu C-L, Tai C-S, Fu L-C. Demand-side management in residential community realizing sharing economy with bidirectional PEV while additionally considering commercial area. Int J Electr Power Energy Syst 2020;116:105512.
[30] Ahmed EM, Rathinam R, Dayalan S, Fernandez GS, Ali ZM, Aleem SHEA, et al. A comprehensive analysis of demand response pricing strategies in a smart grid environment using particle swarm optimization and the strawberry optimization algorithm. Mathematics 2021;9:2338.
[31] Li Y, Han M, Yang Z, Li G. Coordinating flexible demand response and renewable uncertainties for scheduling of community-integrated energy systems with an electric vehicle charging station: a bi-level approach. IEEE Trans Sustain Energy 2021;12:2321–31.
[32] Tamilarasu K, Sathiasamuel CR, Joseph JDN, Elavarasan RM, Mihet-Popa L. Reinforced demand side management for educational institution with incorporation of user's comfort. Energies 2021;14:2855.
[33] Venkatesh B, Sankaramurthy P, Chokkalingam B, Mihet-Popa L. Managing the demand in a micro grid based on load shifting with controllable devices using hybrid WFS2ACSO technique. Energies 2022;15:790.
[34] Venkatesh B, Padmini S. Managing the smart grid with demand side management using Antlion Optimization. Lect Notes Electr Eng 2022;795:313–22.
[35] Mohseni S, Brent AC, Burmester D, Browne WN. Lévy-flight moth-flame optimisation algorithm-based micro-grid equipment sizing: an integrated investment and operational planning approach. Energy AI 2021;3:100047.
[36] Ramli MAM, Bouchekara HREH, Alghamdi AS. Optimal sizing of PV/wind/diesel hybrid microgrid system using multi-objective self-adaptive differential evolution algorithm. Renew Energy 2018;121:400–11.
[37] Ahmad G, Enayatzare M. Optimal energy management of a renewable-based isolated microgrid with pumped-storage unit and demand response. Renew Energy 2018;123:460–74.
[38] Wu K, Zhou H, An S, Huang T. Optimal coordinate operation control for wind-photovoltaic-battery storage power generation units. Energy Convers Manag 2015; 90:466–75.
[39] Malheiro A, Castro PM, Lima RM, Estanqueiro A. Integrated sizing and scheduling of wind/PV/diesel/battery isolated systems. Renew Energy 2015;83:646–57.
[40] Singh S, Singh M, Kaushik SC. Feasibility study of an islanded microgrid in rural area consisting of PV, wind, biomass and battery energy storage system. Energy Convers Manag 2016;128:178–90.
[41] Jasim AM, Jasim BH, Kraiem H, Flah A. A multi-objective demand/generation scheduling model-based microgrid energy management system. Sustainability 2022;14:10158.
[42] Jasim AM, Jasim BH, Bureš V. A novel grid-connected microgrid energy management system with optimal sizing using hybrid grey wolf and cuckoo search optimization algorithm. Front Energy Res 2022;10:960141.
[43] Jasim AM, Jasim BH. Grid-forming and grid-following based microgrid inverters control. Iraqi J Electr Electr Eng 2022;18(1).
[44] Rahbari-asr N, Zhang Y, Chow M-Y. Cooperative distributed scheduling for storage devices in microgrids using dynamic KKT multipliers and consensus networks. In: IEEE Power and Energy Society General Meeting; 2015.
[45] Rahbari-Asr N, Zhang Y, Chow M-Y. Consensus-based distributed scheduling for cooperative operation of distributed energy resources and storage devices in smart grids. IET Gener Trans Distrib 2016;10(5):1268–77.
[46] Singh AK, Singh R, Pal BC. Stability analysis of networked control in smart grids. IEEE Trans Smart Grid 2015;6(1):381–90.
[47] Olfati-Saber R, Fax JA, Murray RM. Consensus and cooperation in networked multi-agent systems. Proc IEEE 2007;95(1):215–33.
[48] Jaderyan M, Khotanlou H. Virulence optimization algorithm. Appl Soft Comput 2016;43:596–618.
[49] Alizon S, Hurford A, Mideo N, Van Baalen M. Virulence evolution and the trade-off hypothesis: history, current state of affairs and the future. J Evolution Biol 2009;22 (2):245–59.
[50] Astier S, Albouy J, Moury V, Robaglia C, Lecoq H. Principles of plant virology, genome, pathogenicity, virus ecology. 1st edition. Science Pub Inc; 2008.
[51] Domingo E, Parrish CR, Holland JJ. Origin and evolution of viruses. Academic Press; 2008.
[52] Leppard K, Dimmock N, Easton A. Introduction to modern virology. Blackwell Publishing Limited; 2007.
[53] Mahy WJ, Van Regenmortel MHV. Desk encyclopedia of general virology. Oxford Academic Press; 2009.
[54] Wang GG, Deb S, Coelho LDS. Earthworm optimization algorithm: a bioinspired metaheuristic algorithm for global optimization problems. Int J BioInspired Comput 2018;12(1):1–22.
[55] Ali M, Abid S, Ghafar A, Ayub N, Arshad H, Khan S, et al. Earth worm optimization for home energy management system in smart grid. In: the *12th International Conference on Broad-Band Wireless Computing, Communication and Applications*; 2017.
[56] Ghosh I. Solution of multi-objective optimal power flow using earthworm optimization algorithm. Int J Sci Eng Res 2018;9(9).
[57] Pasupuleti VR, Balaswamy C. Performance analysis of fractional earthworm optimization algorithm for optimal routing in wireless sensor networks. AI Endorsed Trans Scalable Inform Syst 2021;8(32).